

ASYMPTOTICS OF BIVARIATE GENERATING FUNCTIONS WITH
ALGEBRAIC SINGULARITIES

Torin Greenwood

A DISSERTATION

in

Mathematics

Presented to the Faculties of the University of Pennsylvania

in

Partial Fulfillment of the Requirements for the

Degree of Doctor of Philosophy

2015

Supervisor of Dissertation

Robin Pemantle, Merriam Term Professor of Mathematics

Graduate Group Chairperson

David Harbater, Professor of Mathematics

Dissertation Committee:

Robin Pemantle, Merriam Term Professor of Mathematics

Jim Haglund, Professor of Mathematics

Philip Gressman, Professor of Mathematics

ABSTRACT
ASYMPTOTICS OF BIVARIATE GENERATING FUNCTIONS WITH ALGEBRAIC
SINGULARITIES

Torin Greenwood
Robin Pemantle, Advisor

Flajolet and Odlyzko (1990) derived asymptotic formulae the coefficients of a class of univariate generating functions with algebraic singularities. These results have been extended to classes of multivariate generating functions by Gao and Richmond (1992) and Hwang (1996, 1998), in both cases by reducing the multivariate case to the univariate case. Pemantle and Wilson (2013) outlined new multivariate analytic techniques and used them to analyze the coefficients of rational generating functions. In this thesis, we give a brief overview of the new methods Pemantle and Wilson developed. Then, we use these multivariate analytic techniques to find asymptotic formulae for the coefficients of a broad class of bivariate generating functions with algebraic singularities. Beginning with the Cauchy integral formula, we explicitly deform the contour of integration so that it hugs a set of critical points. The asymptotic contribution to the integral comes from analyzing the integrand near these points, leading to explicit asymptotic formulae. Next, we will analyze an example from current research by using this formula. Included in this discussion is a description of how to compute the asymptotics in Maple, including how to implement Gröbner bases.

We then apply multivariate analytic techniques to quantum walks. Bressler and Pemantle (2007) found a $(d + 1)$ -dimensional rational generating function whose coefficients described the amplitude of a particle at a position in the integer lattice after n steps. Here, the minimal critical points form a curve on the $(d + 1)$ -dimensional unit torus. We find asymptotic formulae for the amplitude of a particle in a given position, normalized by the number of steps n , as n approaches infinity. Each critical point contributes to the asymptotics for a specific normalized position. Using Gröbner bases in Maple again, we compute the explicit locations of peak amplitudes. In a scaling window of size \sqrt{n} near the peaks, each amplitude is asymptotic to an Airy function.

Contents

1	Introduction	1
2	Multivariate Analytic Combinatorics of Rational Functions	4
3	Bivariate Analytic Functions with Algebraic Singularities	9
3.1	Historical Background	10
3.2	New Result	12
3.3	Proof Set-Up	14
3.3.1	A Convenient Change of Variables	14
3.3.2	Determining the Quasi-Local Cycle	15
3.3.3	Away from the Quasi-Local Cycle	20
3.4	A Product Integral	22
3.4.1	$(u - p)$ and $(v - q)$ are Small	23
3.4.2	$(v - q)$ or $(u - p)$ is Big	25
3.5	Proof of Theorem	33
3.6	Corollary	39
3.7	Example	40
3.8	Future Research	46

4	Quantum Walks	48
4.1	Introduction	48
4.1.1	Preliminaries	49
4.2	Examples	51
4.2.1	Hadamard QRW	51
4.2.2	Walks with Three or More Chiralities	52
4.2.3	2-dimensional example	54
4.3	Asymptotics	55
4.3.1	Generating Functions	55
4.3.2	Previous Results	57
4.4	Results and Conjectures	58
4.4.1	Computations	61
4.5	Two-dimensional QRW	65
4.6	Next Steps	74
4.6.1	Higher dimensions	74
4.6.2	Multiple peaks	76

Chapter 1

Introduction

Generating functions are a powerful, convenient tool to encode an array of numbers into a single function. Given that a generating function can be computed with limited information about the corresponding array, it is often desirable to learn more about the array from the generating function itself. One particularly useful goal is to approximate the coefficients of a generating function asymptotically as their indices grow in a prescribed way. In particular, if we have a multivariate generating function $F(\mathbf{z})$ with d variables, we will look at the coefficients $[\mathbf{z}^{\mathbf{r}}] F(\mathbf{z})$ as \mathbf{r} approaches infinity along a specified ray in $\mathbb{R}_{\geq 0}^d$.

In Chapter 2 below, we will give a brief outline of the techniques in [PW13] that Pemantle and Wilson developed to tackle multivariate asymptotics. The asymptotic approximations start with the Cauchy integral formula. Pemantle and Wilson describe how to manipulate the cycle of integration so that it is easily analyzed near a set of critical points. These manipulations depend on Morse theory, which determines how far the cycles of integration can be deformed without changing the value of the integral. In the case where the generating function F is rational, Pemantle and Wilson then use residue computations to find explicit asymptotic formulae for the coefficients of the generating functions.

Next, in Chapter 3, we will derive asymptotic formulae for a class of generating functions with

algebraic singularities. While the techniques of Pemantle and Wilson still give the heuristics for how to derive these formulae, we can no longer rely on residue computations because of the branch cuts that come with algebraic singularities. Instead, we find an explicit contour deformation for the domain of integration in the Cauchy integral formula. When this deformation is combined with a change of variables, we will see that the generating function behaves like a binomial function in one variable alone. This enables us to break the bivariate Cauchy integral formula into a product integral near the critical points of the generating function F . After some tedious order-of-magnitude computations, we show that the rest of the domain of integration does not contribute to the integral asymptotically, which gives us our final asymptotic formulae.

Later in Chapter 3, we apply this formula to a generating function from the work of Ron Graham and Fan Chung Graham, based on the Grahams' research which generalizes the cover polynomials of digraphs. In order to analyze the generating function here, we will turn to using Gröbner bases in Maple, which will allow us to find the set of critical points easily. Once the critical points are found, we still must show that they satisfy the conditions we need for the asymptotic formulae to hold. To end Chapter 3, we describe potential research projects for the future.

Finally, in Chapter 4, we look at quantum walks. Quantum walks differ from regular random walks because they allow for destructive interference between different paths connecting the same two locations. This causes particles to spread faster in quantum walks than in regular random walks. In [BP07], Bressler and Pemantle found a $(d + 1)$ -dimensional rational generating function whose coefficients described the amplitude of a particle at any position in the integer lattice after n steps in a quantum walk. These generating functions can be analyzed using the formulae in [PW13]. For a quantum walk in d dimensions, we find a family of minimal critical points, all of which lie on the $(d + 1)$ -dimensional unit torus. By analyzing these critical points, we can approximate the amplitude of a particle at any given position as the number of steps, n , approaches infinity. From here, we can find the location of the peak amplitudes of the quantum walk.

We examine some examples in one dimension, and describe an unusual case where a fake peak

takes much longer to decay than expected. Then, we turn to analyzing walks in two dimensions. Here, the computations become so difficult that we turn to using resultants instead of Gröbner bases, which are too hard to compute in Maple. The chapter ends with a discussion of future projects related to quantum walks, including looking at some three-dimensional walks.

Chapter 2

Multivariate Analytic

Combinatorics of Rational

Functions

In their 2013 book, [PW13], Pemantle and Wilson outline a program which greatly extends the results of previous work on multivariate generating function analysis. Much of the previous research on multivariate asymptotics relied on reducing to the univariate case, and then applying known univariate results to approximate the coefficients of multivariate generating functions. However, in order to reduce to the univariate case, researchers needed to add restrictions to the multivariate generating functions they studied. Pemantle and Wilson avoid relying on univariate results by starting with the multivariate version of the Cauchy integral formula. They begin with a rational function, $F(\mathbf{z}) = G(\mathbf{z})/H(\mathbf{z})$, where G and H are polynomials with real coefficients in the variables z_1, \dots, z_d , and where $F(\mathbf{z})$ is analytic near the origin. We will write $\mathbf{z} = (z_1, \dots, z_d)$ and $\mathbf{z}^{\mathbf{r}} =$

$z_1^{r_1} \cdots z_d^{r_d}$. Then, $F(\mathbf{z})$ has the series representation:

$$F(\mathbf{z}) = \sum_{\mathbf{r} \in \mathbb{N}^d} a_{\mathbf{r}} \mathbf{z}^{\mathbf{r}}$$

The multivariate Cauchy integral formula tells us:

$$[\mathbf{z}^{\mathbf{r}}] F(\mathbf{z}) = \left(\frac{1}{2\pi i} \right)^d \int_T F(\mathbf{z}) \mathbf{z}^{-\mathbf{r}-1} d\mathbf{z} \quad (2.1)$$

Here, the torus T is a product of circles in each complex dimension. T encloses zero, but it does not enclose any singularities of $F(\mathbf{z})$.

In order to approximate the coefficients $a_{\mathbf{r}}$ asymptotically as $\mathbf{r} \rightarrow \infty$, we first need to specify what this means for multivariate generating functions. Here, we will choose some fixed unit vector $\hat{\mathbf{r}} \in \mathbb{R}_{\geq 0}^d$, and we will approximate $[\mathbf{z}^{n\hat{\mathbf{r}}}] F(\mathbf{z})$ as n approaches infinity.

To analyze the Cauchy integral, we will take advantage of the fact that the $\mathbf{z}^{-\mathbf{r}}$ term dominates the integrand as \mathbf{r} approaches infinity. The idea is to expand the torus T until it nears some singularities of $F(\mathbf{z})$. Here, in the case of rational generating functions, the singularities of $F(\mathbf{z})$ are the zero set of $H(\mathbf{z})$. Eventually, the torus will hit some of the singularities of $F(\mathbf{z})$ and become stuck. Depending on how we expand T , we will have a choice as to which singularities T will hit first. So, we expand T to some cycle \mathcal{C} which gets stuck at a chosen set of the singularities of F , and which expands beyond these singularities elsewhere. In the locations where \mathcal{C} nears the singularities of F , we will have \mathcal{C} hug the singular variety $\mathcal{V} := \mathcal{V}_H = \{\mathbf{z} : H(\mathbf{z}) = 0\}$. Due to the $\mathbf{z}^{-\mathbf{r}}$ term in the integrand, we hope that as $\mathbf{r} \rightarrow \infty$, the integrand will decay exponentially faster in the regions of \mathcal{C} away from the singularities of F , since the magnitude of \mathbf{z} is larger in these regions. If this is true, then we can approximate the integral by analyzing the integrand near the singularities, since the rest of the integral decays too quickly to contribute to the asymptotics. Several questions remain unanswered here. First, can we guarantee that the integrand does not decay near the singularities, so that they contribute to the asymptotics? Second, what will the cycle \mathcal{C} look like near the singularities? And, finally, how can we compute the contribution of these singularities to the integral overall? In the end, Pemantle and Wilson compute the residues of

$F(\mathbf{z})z^{-\mathbf{r}-1}$ over cycles near the correct singularities.

To find singularities which contribute to the asymptotics, we aim to minimize the maximum modulus of $\mathbf{z}^{-\mathbf{r}}$ along our contour. The reason for this is as follows: we want to find a contour where the integrand attains its maximum modulus over some small interval, and then decays rapidly away from this interval. If we could find a contour where the maximum modulus had not been minimized, then we would get a much larger estimate than we would by finding a contour where the maximum modulus has been minimized, which would lead to different asymptotic formulae. Additionally, at a point where the maximum modulus is not minimized, the argument of the $\mathbf{z}^{-\mathbf{r}}$ term will oscillate rapidly as \mathbf{r} tends to infinity, which leads to cancellation near the singularity. However, when the maximum modulus is minimized, we will be able to approximate the integral in this region by using saddle point methods.

To minimize the maximum modulus of $\mathbf{z}^{-\mathbf{r}}$, we will consider the height function,

$$h(\mathbf{z}) := h_{\hat{\mathbf{r}}}(\mathbf{z}) := -\hat{\mathbf{r}} \cdot \operatorname{Re} \log \mathbf{z}.$$

Although this excludes the contribution from $F(\mathbf{z})$ in the integrand, $F(\mathbf{z})$ is bounded on compact sets, so h still approximates the log modulus of the integrand as \mathbf{r} approaches infinity in the direction of $\hat{\mathbf{r}}$. Now, knowing that we will expand the torus until it hits a singularity of F so that h will be minimized, we will consider the values of h on \mathcal{V} . On a cycle where the maximum of h is minimized, the points where the maximum of h is attained are saddle points of h . Thus, the critical points of h restricted to \mathcal{V} will be candidates for the singularities that will contribute to the asymptotics.

Before moving on to how to calculate these critical points, we will discuss how to determine the topology of \mathcal{V} near the critical point. This is important, because when we expand T into a contour \mathcal{C} that approaches these singularities, we must know the topology of \mathcal{V} to identify our contour \mathcal{C} . To analyze this, we will rely on Morse theory, with $h(\mathbf{z})$ as our “height function.” Let \mathcal{V}^c be the subset $\{\mathbf{z} \in \mathcal{V} : h(\mathbf{z}) \leq c\}$. We will consider how the topology of \mathcal{V}^c changes as c increases. Every

algebraic variety has a Whitney stratification, so in particular, \mathcal{V} has a Whitney stratification. As described in Goresky and MacPherson’s book on stratified Morse theory, [GM88], the topology of \mathcal{V}^c only changes at the critical values of h . More explicitly, if the interval $[a, b]$ contains no critical values of h , then there is a strong deformation retraction of \mathcal{V}^b onto \mathcal{V}^a . In turn, this implies that any cycle \mathcal{D} supported on \mathcal{V}^b can be carried by this retraction to a cycle supported on \mathcal{V}^a . Hence, when integrating an analytic function over \mathcal{D} , we can push \mathcal{D} to a cycle supported on \mathcal{V}^a without changing the value of the integral. Now, in order to minimize the maximum value of h along a cycle in \mathcal{V} , we can use these retractions to push the cycle “downwards” until the cycle hits a critical point of h and becomes stuck there. Morse theory can describe the topology of \mathcal{V} near the critical points of h . Thus, when \mathcal{D} has been lowered until it becomes stuck around some critical point of h , Morse theory can be used to describe the portion of the cycle that is in a small neighborhood of the critical point itself. This portion of the cycle is called a *quasi-local cycle*.

Unfortunately, we have only discussed cycles within \mathcal{V} itself, but our integral begins with a torus T in $\mathcal{M} = \mathbb{C}^d \setminus \mathcal{V}$. However, there is a dual version of the Morse theoretic statements discussed above which states that the homology classes of \mathcal{M} only change at these same critical points of h . Thus, we will be able to expand T into a cycle \mathcal{C} that approaches the critical points of h , and near the critical point, it looks like the quasi-local cycle described by Morse theory. Now, we can compute the contribution of each critical point to the integral by using residues. However, these residue computations depend on the topology of the quasi-local cycle, leading to different asymptotic formulae for different types of critical points. In Pemantle and Wilson’s book, many different asymptotic formulae are computed for different classes of quasi-local cycles. Once the contribution of each critical point is calculated, the results can be summed to find the final asymptotic formulae, since the critical points are isolated, so that their contributions are independent.

Now, we must return to finding the critical points of h . First, we consider a stratification of the space \mathcal{V}_H , and restrict our attention to critical points within a certain stratum S . Given S , we may write the closure \bar{S} as the intersection of several other varieties $\mathcal{V}_{f_1}, \dots, \mathcal{V}_{f_{d-k}}$, where the

f_j are computable and have non-vanishing gradients at every point of S . Note that while S is the actual stratum, \bar{S} is a k -dimensional variety containing the stratum that may be larger than S .

Let $\mathbf{z} = (z_1, \dots, z_d)$. To find the critical points, we look for where $dh|_{\bar{S}}$ vanishes. $dh|_{\bar{S}}$ vanishing at \mathbf{z} is equivalent to the vector $\hat{\mathbf{r}}$ being in the span of the $d - k$ vectors $\{\nabla_{\log} f_i(\mathbf{z}) : 1 \leq i \leq d - k\}$, where $\nabla_{\log} f(\mathbf{z}) := (z_1 \partial f / \partial z_1, \dots, z_d \partial f / \partial z_d)$ is the gradient of f with respect to $\log \mathbf{z}$. If we let M be the $(d - k + 1) \times d$ matrix whose rows are these $d - k$ gradients and $\hat{\mathbf{r}}$, then at all points of \bar{S} the submatrix of M consisting of the first $d - k$ rows has rank $d - k$. The span of the $d - k$ gradients containing $\hat{\mathbf{r}}$ is equivalent to the vanishing of the k determinants M_{d-k+i} , where M_{d-k+i} contains the first $d - k$ columns of M together with the $(d - k + i)$ th column. This gives the d critical point equations:

$$f_i = 0, \quad \det(M_{d-k+i}) = 0$$

Smooth critical points are a simple yet common special case, where the stratum S is of dimension $k := d - 1$, and $\bar{S} = \mathcal{V}$. Thus, in this case, $f_1 = H = 0$, and the other $d - 1$ equations from above can be rewritten as follows:

$$\begin{aligned} r_1 z_2 \frac{\partial H}{\partial z_2} &= r_2 z_1 \frac{\partial H}{\partial z_1} \\ &\vdots \\ r_1 z_d \frac{\partial H}{\partial z_d} &= r_d z_1 \frac{\partial H}{\partial z_1} \end{aligned}$$

This may be written as $H = 0, \nabla_{\log} H|_{\hat{\mathbf{r}}_*}$. When H is square-free, to check for smoothness at these critical points, we also require that ∇H does not vanish on \mathcal{V} . When H is a polynomial, the above critical point equations form a system of polynomial equations. In this case, Gröbner bases can help compute the critical points. In general, it is not necessarily true that all critical points will contribute to the leading term of the Cauchy integral.

Chapter 3

Bivariate Analytic Functions with Algebraic Singularities

This section concerns generating functions with algebraic singularities and smooth critical points. We will examine functions of the form, $H(x,y)^{-\beta}$, where H is an analytic function with real coefficients and $\beta \in \mathbb{R}$ is not a negative integer. Using the procedure outlined in [PW13], one sees again that the coefficients of $H^{-\beta}$ are well-approximated by the sum of integrals over quasi-local cycles around the critical points of the function H . However, instead of computing the residues of the remaining integrals, we use classical contour deformations and analyze the integrand directly. Hankel contours historically enabled the analysis of integrals in domains with branch cuts. Here, we will use a modified version of such a contour, and we will show that $H^{-\beta}$ is well-approximated by a one-dimensional binomial function over part of this contour. This one-dimensional function is easy to integrate, giving us the main result stated in section 3.2 below.

3.1 Historical Background

Work on asymptotic approximations of generating functions with algebraic singularities began with univariate generating functions, which encode sequences of numbers. In 1990, Flajolet and Odlyzko, [FO90], described how to compute the asymptotics of a class of univariate generating functions with algebraic singularities. In particular, they considered functions of the form,

$$g(z) = K(1 - z)^\alpha (\log(1 - z))^\gamma (\log \log(1 - z))^\delta, \quad (3.1)$$

where α, γ, δ , and K are arbitrary real numbers. They also considered related classes of functions, which were again the products and compositions of power functions and logarithms. Their results differed from previous results both in the class of generating functions covered, and in their method of proof. Because we will use similar techniques in our proofs later, we take a moment to summarize their proof here. Flajolet and Odlyzko relied on the univariate Cauchy integral formula:

$$[z^n]g(z) = \frac{1}{2\pi i} \int_{\mathcal{C}} g(z) \frac{dz}{z^{n+1}}$$

Here, $[z^n]g(z)$ represents the coefficient of z^n in the power series expansion of g , and \mathcal{C} is any positively-oriented contour around the origin which does not enclose any singularities of $g(z)$. Starting with any function f such that $f(z) = O(|1 - z|^\alpha)$ as $z \rightarrow 1$, and letting \mathcal{C} be a small circle around the origin, the authors expanded \mathcal{C} in hopes of finding a contour which is easier to analyze. As \mathcal{C} expands, it must avoid not only the singularity at 1, but also the branch cut emanating from this point. They expand the contour so it looks like a Hankel contour, \mathcal{C}^* , as shown in Figure 3.1.

Flajolet and Odlyzko also require the extra assumption that g is analytic within the contour \mathcal{C}^* , which ensures that the original contour could be expanded to \mathcal{C}^* . From here, the contour is broken up into segments, $\gamma_1, \gamma_2, \gamma_3$, and γ_4 . As n approaches infinity, $g(z)/z^{n+1}$, the integrand in Cauchy's integral formula, decays exponentially faster on γ_4 than it does on γ_1 . For this reason, the integral over γ_4 is negligible in the asymptotic expression of $[z^n]g(z)$. Likewise, the contribution along most of γ_2 and γ_3 is negligible, meaning that the asymptotics of $[z^n]g(z)$ are controlled by

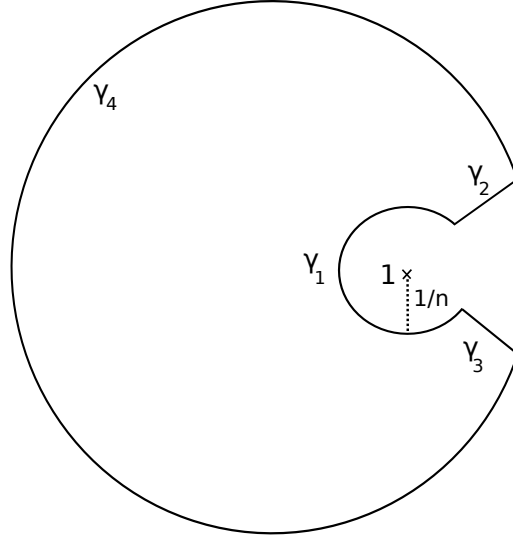


Figure 3.1: The expanded contour, \mathcal{C}^* , used in Flajolet and Odlyzko's proof.

the integrand near $z = 1$. However, near $z = 1$, $f(z) = O(|z-1|^\alpha)$, which means that f is bounded along the contours near the critical point, leading to the bound, $[z^n]f(z) = O(n^{-\alpha-1})$. Then, they expanded their results to functions $g(z)$ with the form in (3.1).

Later in the 1990s, other researchers extended these results to classes of multivariate generating functions. Bender and Richmond, [BR83], had already considered the asymptotics of multivariate generating functions with poles in 1983. In 1992, Gao and Richmond, [GR92], considered classes of bivariate generating functions $F(z, x)$ which are of a form they called algebraico-logarithmic, which includes some generating functions with algebraic singularities. The convenience of algebraico-logarithmic functions is that by considering $[z^n]F(z, x)$ and temporarily fixing x , the problem is reduced to a univariate generating function where the results of Flajolet and Odlyzko can be applied. Then, the asymptotic approximations for $[z^n]F(z, x)$ can be broken down further to approximate the coefficients $[z^n x^k]F(z, x)$.

In his 1996 and 1998 papers, [Hwa96] and [Hwa98], Hwang expanded upon the multivariate results, using a probability framework and deriving large deviation theorems. In 1996, Hwang considered sequences of random variables $\{X_n\}$. Assuming that the moment generating functions

of the X_n were of a particular form, Hwang proved a central limit theorem for $\{X_n\}$. Then, he considered a class of bivariate generating functions $P(w, z)$ such that after approximating $[z^n]P(w, z)$ with Flajolet and Odlyzko's univariate results, $[z^n]P(w, z)$ satisfied the same conditions he required previously of the moment generating functions of Ω_n . Applying his central limit theorem from before gave asymptotic results for a new class of bivariate generating functions. In 1998, Hwang extended his results by using univariate saddle point methods to approximate integrals.

3.2 New Result

Let us summarize notation in a bivariate setting. Let \mathcal{V} be the zero set of the analytic function, $H(x, y)$, where $H(0, 0) \neq 0$. We will approximate the coefficients $[x^r y^s] H(x, y)^{-\beta}$ for a fixed $\beta \in \mathbb{R}$ as r and s approach infinity with their ratio approaching the constant, λ . Critical points in the direction of $\lambda = \frac{r+O(1)}{s}$ (as r and s approach infinity) are defined to be the points (p_i, q_i) where the following equations hold:

$$\begin{aligned} H &= 0 \\ ry \frac{\partial H}{\partial y} &= sx \frac{\partial H}{\partial x} \end{aligned}$$

We call the critical points smooth if ∇H does not vanish on \mathcal{V} at the critical points. Let \mathcal{D} be the domain of convergence of the power series of $H^{-\beta}$ that converges around the origin, $(0, 0)$. Then, a critical point (p, q) is called minimal if $(p, q) \in \partial\mathcal{D}$. We will apply heuristics from Chapter 2 to prove the following result about bivariate generating functions with algebraic singularities:

Theorem 3.2.1. *Let H be an analytic function with exactly n strictly minimal critical points $\{(p_i, q_i)\}_{i=1}^n$, all of which are smooth and lie on the same torus T^* . (Hence, $|p_i| = |p_j|$ and $|q_i| = |q_j|$ for all $1 \leq i, j \leq n$.) Let $\beta \in \mathbb{R}$ with $\beta \notin \mathbb{Z}_{\leq 0}$, and let $\lambda = \frac{r+O(1)}{s}$ as $r, s \rightarrow \infty$. Define*

χ_1, χ_2 , and M_i as follows:

$$\begin{aligned}\chi_1 &= \frac{H_y(p_i, q_i)}{H_x(p_i, q_i)} = \frac{p}{\lambda q} \\ \chi_2 &= \frac{1}{2H_x}(\chi_1^2 H_{xx} - 2\chi_1 H_{xy} + H_{yy}) \Big|_{(x,y)=(p_i, q_i)} \\ M_i &= -\frac{2\chi_2}{p_i} - \frac{\chi_1^2}{p_i^2} - \frac{1}{\lambda q_i^2}\end{aligned}$$

For all i , assume $p_i, q_i, H_x(p_i, q_i)$, and M_i are nonzero, and assume that the real part of $-q^2 M$ is strictly positive. Define $\{x^{-\beta}\}_P$ as the value of $x^{-\beta}$ defined by using a ray from the origin of \mathbb{C} as the branch cut of the logarithm. In this definition, choose any ray such that $\{H(x, y)^{-\beta}\}_P = H(x, y)^{-\beta}$ in a neighborhood of the origin in \mathbb{C}^2 (as defined by the power series of $H^{-\beta}$), and such that this ray does not pass through $-p_i H_x(p_i, q_i)$ for any i . Let ω_i be the signed number of times the curve $H(tp_i, tq_i)$ crosses this branch cut in a counterclockwise direction as t increases, $0 \leq t < 1$. Then, the following expression holds as $r, s \rightarrow \infty$:

$$[x^r y^s] H(x, y)^{-\beta} = \sum_{i=1}^n \frac{r^{\beta-\frac{3}{2}} p_i^{-r} q_i^{-s} \{(-H_x(p_i, q_i) p_i)^{-\beta}\}_P e^{-\beta(2\pi i \omega_i)}}{\Gamma(\beta) \sqrt{-2\pi q_i^2 M_i}} + o\left(r^{\beta-\frac{3}{2}} p_1^{-r} q_1^{-s}\right)$$

Here, the square root in the denominator is taken to be the principal root.

To prove this result, we analyze the multivariate Cauchy integral formula, (2.1). The dominating contributions to this integral come over quasi-local cycles centered at each critical point, since the height function h decays exponentially away from these points. Because the critical points are discrete, we can analyze them individually. An outline of the analysis is as follows: we will show that $H(x, y)$ behaves essentially as a linear function in one variable, with some minor error terms in the second variable. In order to do this, we will need to introduce a change of variables, (u, v) , which will give us a particularly nice power series expansion of H in u and v . This change of variables is what determines χ_1 and χ_2 . Next, we will justify approximating the resulting integral by an iterated integral, relying on the fact that H is nearly linear. This step is by far the most tedious, and will take many lemmas to justify. Finally, we will analyze this iterated integral.

Note that it is possible to use Morse theory to show that any zeroes of H on $\partial\mathcal{D}$ must be critical

points. Additionally, when all the minimal critical points are smooth, they must contribute to the leading term asymptotics of the coefficients of H , which forces each pair (p_i, q_i) to contribute a term of equal order in r and s to the asymptotics in the theorem.

3.3 Proof Set-Up

3.3.1 A Convenient Change of Variables

In order to approximate $H(x, y)$ as a univariate linear function near the critical point (p, q) , we will need the power series expansion of H to have no constant term, linear term, nor quadratic term in one of its two input variables. (We will prove that this condition allows us to approximate H as a univariate linear function later.) With this goal in mind, we define the following change of variables:

$$\begin{aligned} u &= x + \chi_1(y - q) + \chi_2(y - q)^2 \\ v &= y \end{aligned}$$

Here, χ_1 and χ_2 are as defined in Theorem 3.6.1 above. Write H as a power series in u and v :

$$H(x, y) = \sum_{m, n \geq 0} d_{mn} (u - p)^m (v - q)^n =: \tilde{H}(u, v)$$

Since $H(p, q) = 0$, we have that $d_{00} = 0$. Notice that when $(x, y) = (p, q)$, we also have that $(u, v) = (p, q)$. We can check that $d_{01} = d_{02} = 0$:

$$\begin{aligned} \frac{\partial H}{\partial v} \Big|_{(u,v)=(p,q)} &= \left(\frac{\partial H}{\partial x} \cdot \frac{\partial x}{\partial v} + \frac{\partial H}{\partial y} \cdot \frac{\partial y}{\partial v} \right) \Big|_{(x,y)=(p,q)} \\ &= H_x \cdot (-\chi_1 - 2\chi_2(v - q)) + H_y \Big|_{(u,v)=(p,q)} \\ &= -\chi_1 H_x + H_y \Big|_{(u,v)=(p,q)} \\ &= 0 \end{aligned}$$

$$\begin{aligned}
\left. \frac{\partial^2 H}{\partial v^2} \right|_{(u,v)=(p,q)} &= -2\chi_2 H_x + (-\chi_1 - 2\chi_2(v-q)) \left[H_{xx} \frac{\partial x}{\partial v} + H_{xy} \frac{\partial y}{\partial v} \right] \\
&\quad + H_{xy} \frac{\partial x}{\partial v} + H_{yy} \frac{\partial y}{\partial v} \Big|_{(u,v)=(p,q)} \\
&= -2\chi_2 H_x + \chi_1^2 H_{xx} - 2\chi_1 H_{xy} + H_{yy} \Big|_{(u,v)=(p,q)} \\
&= 0
\end{aligned}$$

Thus, $\tilde{H}(u, v) = \sum_{m,n \geq 0} d_{mn} (u-p)^m (v-q)^n$ with $d_{00} = d_{01} = d_{02} = 0$.

3.3.2 Determining the Quasi-Local Cycle

For now, assume that there is a unique critical point, (p, q) . Recall that the original domain of integration in (2.1) is a torus T around the origin which encloses no singularities of $H^{-\beta}(x, y)$. To decrease the magnitude of the integrand exponentially as r and s approach infinity, we will expand the torus T towards the minimal critical point, (p, q) . Because (p, q) is a strict minimal critical point, there cannot be any zeroes between the origin and (p, q) that would otherwise obstruct the deformation. Hence, we can expand the domain of integration through a homotopy until it is near the critical point. Previous work on generating functions with poles relied on computing residues, but the branch point created by algebraic singularities forces us to use explicit contour deformations through homotopies here. In order to expand the domain of integration past the critical points of a generating function with algebraic singularities, we must view the contours as on the Riemann surface of the generating function. However, we will provide explicit contour deformations, as in Figures 3.2 and 4.8, so it is not necessary to understand the general method here.

Before expanding the torus, T is the product of a small x circle and a small y circle. To begin deforming the torus, expand the y circle until it becomes the circle, $|y| = |q|$. The y portion of the quasi-local cycle, \mathcal{C}_y , will be the part of this circle where $y = qe^{i\theta}$ for $|\theta| \leq \theta_y$ for some constant $\theta_y > 0$ that will be restricted further later. It is pictured in Figure 3.2.

Now, for each $y \in \mathcal{C}_y$, we will expand the x circle until it approaches the zero set of H near p .

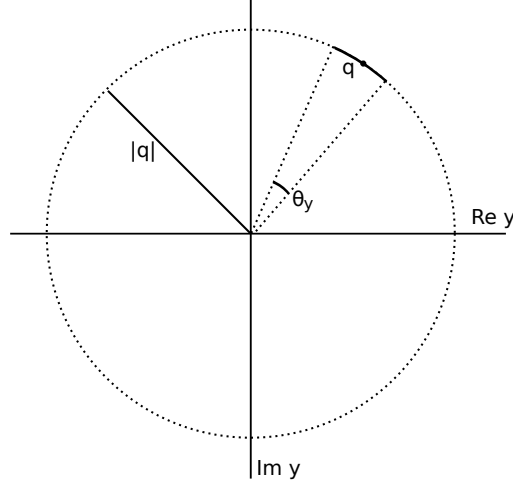


Figure 3.2: The y portion of the quasi-local contour

When y is close to q , we will wrap the x contour around the zero set of H . However, when y is further away from q , we will expand the x contour less, so that it does not come into contact with the zero set of H .

More explicitly, since $H_x(p, q) \neq 0$ and H is analytic, the implicit function theorem guarantees that we can parameterize the variety $\mathcal{V} = \{(x, y) | H(x, y) = 0\}$ by a smooth function $G(y)$, so that $H(p + G(y), y) = 0$ for all $y \in \mathcal{C}_y$ with θ_y sufficiently small. So, for $y = qe^{i\theta}$ with $|\theta| \leq \frac{\theta_y}{2}$, we choose the x contour in Figure 4.8.

The equations for the pieces of the contour are as follows:

$$\begin{aligned} \gamma_1(y) &:= \left\{ x : |x - p - G(y)| = \frac{1}{r}, \arg(p) \leq \arg(x - p - G(y)) \leq \arg(p) + 2\pi \right\} \\ \gamma_2(y) &:= \left\{ x : \frac{1}{r} \leq |x - p - G(y)| \leq \epsilon_x, \arg(x - p - G(y)) = \arg(p) + 2\pi \right\} \\ \gamma_3(y) &:= \left\{ x : \frac{1}{r} \leq |x - p - G(y)| \leq \epsilon_x, \arg(x - p - G(y)) = \arg(p) \right\} \\ \gamma_4(y) &:= \{ x : |x - G(y)| = |p| + \epsilon_x, \arg(p) - \theta_x \leq \arg(x - G(y)) \leq \arg(p) \} \\ \gamma_5(y) &:= \{ x : |x - G(y)| = |p| + \epsilon_x, \arg(p) \leq \arg(x - G(y)) \leq \arg(p) + \theta_x \} \end{aligned}$$

Here, ϵ_x and $\theta_x > 0$ are positive real numbers that are small enough that the contour hits no other zeroes of H and so that $G(y)$ is a valid parameterization of the zero set of H around this

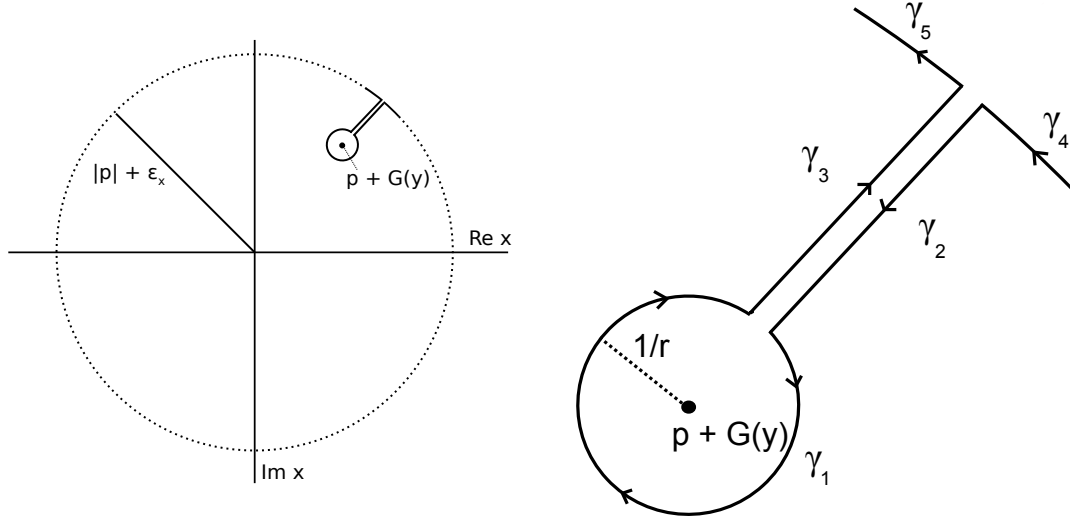


Figure 3.3: The x contour on the left, and a close up of the contour on the right.

contour. (This is possible by the implicit function theorem. We will add more restrictions to both ϵ_x and θ_x later.) In the contour above, the inner and outer rays γ_2 and γ_3 are directly on top of each other, but they have differing arguments. These segments should be viewed as different segments on the Riemann surface of $H^{-\beta}$. However, the magnitude of the integrand will be the same on γ_2 and γ_3 , and hence the difference in argument has no impact in the order-of-magnitude computations below. Thus, we will not talk about the impact of the differing arguments until the end of the proof, in Section 3.5 below. Before this discussion, we treat the argument as a value modulo 2π .

Consider the case where $|\theta| \geq \frac{\theta_y}{2}$. As θ increases, we must extricate the x contours from \mathcal{V} . To do this, we will gradually shrink the outer radius of the x contours – that is, the radius $|p| + \epsilon_x$ in $\gamma_4(y)$ and $\gamma_5(y)$ will shrink until the contour no longer wraps around \mathcal{V} .

To do this, notice that when $y = qe^{i\theta_y t}$ for $t \in [-1, -\frac{1}{2}] \cup [\frac{1}{2}, 1]$, $|p + G(y)| > |p|$ uniformly, since (p, q) is a strictly minimal critical point of H . Therefore, we can find a $\delta > 0$ so that $|p + G(y)| > |p| + \delta$ for every $t \in [-1, -\frac{1}{2}] \cup [\frac{1}{2}, 1]$.

We will linearly interpolate the radius $|x - G(y)|$ in γ_4 and γ_5 from $|p| + \epsilon_x$ to $|p| + \delta$, knowing

that reducing the radius to $|p| + \delta$ will completely remove the contour from the zero set of H . Writing $y = qe^{i\theta_y t}$ with $t \in [-1, -\frac{1}{2}] \cup [\frac{1}{2}, 1]$, we define the following radial interpolation with respect to t :

$$R(t) := (2 - 2|t|) \cdot [|p| + \epsilon_x] + (2|t| - 1) \cdot [|p| + \delta]$$

Then, for y with $\theta \geq \frac{\theta_y}{2}$, we define γ_4 and γ_5 as follows:

$$\gamma_4(q + tc) := \{x : |x - G(y)| = R(t), \arg(p) - \theta_x \leq \arg(x - G(y)) \leq \arg(p)\}$$

$$\gamma_5(q + tc) := \{x : |x - G(y)| = R(t), \arg(p) \leq \arg(x - G(y)) \leq \arg(p) + \theta_x\}$$

As $R(t)$ shrinks, γ_2 and γ_3 will shorten until they no longer are part of the contour. When this happens, γ_1 will partially intersect γ_4 and γ_5 until it moves completely out of the contour as well, leaving behind just an arc. We will show that the integrand is small along all parts of this contour, so the details of these intersections are not important.

This completes the description of a possible quasi-local contour near (p, q) , but we will morph it slightly so that it is more convenient. Consider applying the change of variables given in Section 3.3.1. Since $v = y$, the v portion of the contour is identical to the y portion of the contour. Then, since $u = x + \chi_1(v - q) + \chi_2(v - q)^2$, each contour $\gamma_i(y)$ is translated by $\chi_1(v - q) + \chi_2(v - q)^2$, so that it retains its overall shape but is centered at a new location.

Using the chain rule, we compute the following:

$$\begin{aligned} \left. \frac{\partial \tilde{H}}{\partial u} \right|_{(u,v)=(p,q)} &= \left. \frac{\partial H}{\partial x} \cdot \frac{\partial x}{\partial u} + \frac{\partial H}{\partial y} \cdot \frac{\partial y}{\partial u} \right|_{(x,y)=(p,q)} \\ &= H_x(p, q) \end{aligned} \tag{3.2}$$

Since $H_x(p, q) \neq 0$ by assumption, and since \tilde{H} is analytic, the implicit function theorem guarantees that there exists a smooth parameterization $\kappa(v)$ of the zero set of \tilde{H} , so that $\tilde{H}(p + \kappa(v), v) = 0$ for v sufficiently close to q . Investigating $\kappa(v)$ a little further, we use the power series expansion

of \tilde{H} about (p, q) to obtain the following:

$$0 = \tilde{H}(p + \kappa(v), v) = d_{10}\kappa(v) + O(\kappa(v))^2 + O(v - q)^3$$

Thus, $\kappa(v) = O(v - q)^3$. Additionally, the definitions of $G(y)$, $\kappa(v)$, and the change of variables give us the following relation:

$$0 = H(p + G(y), y) = \tilde{H}(p + G(v) + \chi_1(v - q) + \chi_2(v - 2)^2, v)$$

However, we know already that $\kappa(v)$ is the parameterization of the zero set of \tilde{H} . This forces the following relation:

$$G(y) = \kappa(y) - \chi_1(y - q) - \chi_2(y - q)^2$$

Hence, $G(y) = -\chi_1(y - q) - \chi_2(y - q)^2 + O(v - q)^3$. This provides more insight into this change of variables: in addition to allowing us to write H as a nice power series with some vanishing coefficients, the change of variables also describes \mathcal{V} near (p, q) . By converting the contour into (u, v) -coordinates, we are able to stabilize the u contours, slowing down the movement of the zero set of H when it is parameterized by v . We take advantage of this slow-down by morphing our contour slightly, as described in the following paragraph.

In order to break the 2-dimensional Cauchy integral into two one-dimensional integrals, we need the quasi-local contour to be a product contour near the critical point, (p, q) . To achieve this goal, we will need to break into two cases: when $|\theta| \leq r^{-\frac{2}{5}}$ and when $|\theta| > r^{-\frac{2}{5}}$, for $v = qe^{i\theta}$. Let us first analyze $|v - q|$ in these cases.

$$\begin{aligned} v - q &= qe^{i\theta} - q \\ &= q(e^{i\theta} - 1) \\ &= q(1 + i\theta - \theta^2 + O(\theta)^3 - 1) \\ &= qi\theta - \frac{q\theta^2}{2} + O(\theta)^3 \end{aligned} \tag{3.3}$$

In the third line, we use the power series expansion for e^x , which holds uniformly as $\theta \rightarrow 0$. Now, if $|\theta| \leq r^{-\frac{2}{5}}$, then $|(v - q)^3| = O\left(r^{-\frac{6}{5}}\right) < \frac{1}{r}$ for r sufficiently large. Hence, when $|\theta| \leq r^{-\frac{2}{5}}$,

$|\kappa(v)| = O\left(r^{-\frac{6}{5}}\right)$. Therefore, for r sufficiently large, the point $p + \kappa(v)$ is always within the circle of radius $\frac{1}{r}$ about the point p , and we can morph our u -contour so that it is centered exactly around the point p instead of the point $p + \kappa(v)$. Thus, we will drop $\kappa(v)$ from the definitions of all the γ_i when $\theta \leq r^{-\frac{2}{5}}$, which means that the u contour no longer depends on v when $\theta \leq r^{-\frac{2}{5}}$. (Note that this corresponds to a similar shift in the original (x, y) -coordinates, which can be computed explicitly to justify that the original torus T can be morphed locally to this new contour.) The portion of the contour where $\theta \leq r^{-\frac{2}{5}}$ will yield the dominating contribution to the integral asymptotically.

In the other regime, when $\theta \geq r^{-\frac{2}{5}}$, we cannot simply eliminate $\kappa(v)$. Instead, let $\tilde{\kappa}(v)$ be 0 when $\theta \leq r^{-\frac{2}{5}}$, let it be $\kappa(v)$ when $\theta \geq r^{-\frac{7}{20}}$, and let it linearly interpolate between 0 and $\kappa(v)$ when $r^{-\frac{2}{5}} \leq \theta \leq r^{-\frac{7}{20}}$. We replace $\kappa(v)$ with $\tilde{\kappa}(v)$ in the definition of the quasi-local cycle. Note that $\tilde{\kappa}(v) = O(v - q)^3$ as v tends to q . This condition will be used much later in the proof.

In summary, the final quasi-local cycle $\mathcal{C}(p, q)$ (in (u, v) -coordinates) near the critical point (p, q) has three regimes. The contour is an arc in v , and wraps around the zero set of \tilde{H} in u . When $\theta \leq r^{-\frac{2}{5}}$, the u -contour wraps exactly around the point, p , and this portion of the contour is a product contour. When $r^{-\frac{2}{5}} \leq \theta \leq \frac{\theta_y}{2}$, the contour instead wraps around the point, $p + \tilde{\kappa}(v)$. Finally, if $\theta \geq \frac{\theta_y}{2}$, then the u -contour gradually shrinks as θ increases, until it no longer intersects the zero set of \tilde{H} at all.

3.3.3 Away from the Quasi-Local Cycle

Let us justify that the integral over the quasi-local cycle provides the main contribution to the asymptotics of the coefficients. In order to do so, we will find a way to expand the torus T away from the quasi-local cycle so that the integrand decays exponentially faster here when compared to the quasi-local cycle. To begin, consider the case where there is only one strictly minimal critical

point, (p, q) . Formally, by strictly minimal, we mean the following:

$$\{|x| \leq |p|\} \cap \{|y| \leq |q|\} \cap \mathcal{V}_H = (p, q)$$

Here again, $\mathcal{V}_H = \{(x, y) | H(x, y) = 0\}$.

Consider the torus, $T_{(p,q)} := \{x : |x| = |p|\} \times \{y : |y| = |q|\}$. From this torus, remove an open neighborhood \mathcal{N} of the point (p, q) , where \mathcal{N} is so small that the angular sectors of the torus that it covers in x and y are smaller than the angular sectors of the torus that \mathcal{C} covers in x and y . That is, the y component of \mathcal{N} should only consist of y values whose arguments $|\arg(y) - q| < c < \theta_y$ for some constant $c > 0$. Similarly, for each $y \in \mathcal{C}$, the arguments of the x values in \mathcal{N} should not vary from $p + G(y)$ more than the arguments of the x values in \mathcal{C} . Now, $T_{(p,q)} \setminus \mathcal{N}$ is a closed set which does not intersect the closed set, \mathcal{V}_H . Thus, there are open sets dividing these two sets. This implies that there is a neighborhood of $T_{(p,q)} \setminus \mathcal{N}$ which does not intersect \mathcal{V}_H . There is some $\delta^* > 0$ such that the x arc of $T_{(p,q)} \setminus \mathcal{N}$ can be expanded by δ^* without hitting \mathcal{V}_H .

Then, at every point of this new cycle away from the critical point (p, q) , we have that $|x| \geq |p| + \delta^*$. This forces the Cauchy integral to decay exponentially faster away from the critical point than it does near (p, q) , proving that the asymptotic contribution to the integral cannot come from $T_{(p+\delta^*, q)}$.

After expanding $T_{(p,q)}$ to $T_{(p+\delta^*, q)} := \{x : |x| = |p| + \delta^*\} \times \{y : |y| = |q|\}$, notice that $T_{(p+\delta^*, q)} \setminus \mathcal{N}$ can be connected to the quasi-local cycle \mathcal{C} by adding two short lines at the ends of the x contours connecting the circle of radius δ^* to the ends of γ_4 and γ_5 . Because these lines are contained entirely within the region near (p, q) where the implicit function theorem holds for $G(y)$, the lines cannot hit any zeroes of H . Also, the magnitude of $|xy^{\frac{1}{\lambda}}|$ along these lines is always greater than the magnitude of $|pq^{\frac{1}{\lambda}}|$ because $|x| > |p|$, which means that these lines also do not contribute to the asymptotics of the integral, and may be ignored.

3.4 A Product Integral

After applying the change of variables to the Cauchy integral formula (2.1) restricted to the quasi-local cycle near (p, q) , we obtain the following integral:

$$\left(\frac{1}{2\pi i}\right)^2 \iint_{\mathcal{C}(p,q)} \tilde{H}(u, v)^{-\beta} (u - \chi_1(v - q) - \chi_2(v - q)^2)^{-r-1} v^{-s-1} du dv$$

Here, the Jacobian of the transformation is just 1:

$$\begin{vmatrix} \frac{\partial x}{\partial u} & \frac{\partial x}{\partial v} \\ \frac{\partial y}{\partial u} & \frac{\partial y}{\partial v} \end{vmatrix} = \begin{vmatrix} 1 & -\chi_1 - 2\chi_2(v - q) \\ 0 & 1 \end{vmatrix} = 1$$

As mentioned above, our goal is to show that this integral is essentially a product integral. The following lemma describes this precisely.

Lemma 1.

$$\begin{aligned} & \left(\frac{1}{2\pi i}\right)^2 \iint_{\mathcal{C}(p,q)} \tilde{H}(u, v)^{-\beta} (u - \chi_1(v - q) - \chi_2(v - q)^2)^{-r-1} v^{-s-1} du dv \\ & \sim \left(\frac{1}{2\pi i}\right)^2 \iint_{\mathcal{C}_\ell(p,q)} [H_x(p, q) \cdot (u - p)]^{-\beta} u^{-r-1} v^{-s-1} \left[1 - \frac{\chi_1(v - q) + \chi_2(v - q)^2}{p}\right]^{-r-1} du dv \end{aligned}$$

The above estimate holds as $r, s \rightarrow \infty$ with $\lambda = \frac{r+O(1)}{s}$. Here, $\mathcal{C}_\ell(p, q)$ is the portion of $\mathcal{C}(p, q)$ where $|\theta| \leq r^{-\frac{2}{3}}$. Hence, $\mathcal{C}_\ell(p, q)$ is a product contour.

The proof of this lemma will involve two types of statements: near the critical point, where $|u - p|$ and $|v - q|$ are both sufficiently small, we will argue that the integrands are asymptotically the same. Away from the critical point, where at least one of $|u - p|$ or $|v - q|$ is sufficiently large, we will show that both integrands are small, and hence do not contribute asymptotically to either integral. (In the second integral, we need only show that the integrand is small when $|u - p|$ is large, since $|v - q|$ is always small in $\mathcal{C}_\ell(p, q)$.)

3.4.1 $(u - p)$ and $(v - q)$ are Small

In order to match the two integrands when $|v - q|$ and $|u - p|$ are small, we rewrite the original integrand first:

$$\begin{aligned} & \tilde{H}(u, v)^{-\beta} (u - \chi_1(v - q) - \chi_2(v - q)^2)^{-r-1} v^{-s-1} \\ &= [H_x(p, q) \cdot (u - p)]^{-\beta} u^{-r-1} v^{-s-1} \left[1 - \frac{\chi_1(v - q) + \chi_2(v - q)^2}{p} \right]^{-r-1} K(u, v) L(u, v) \end{aligned}$$

Here, K and L are correction factors with the following definitions:

$$\begin{aligned} K(u, v) &:= \left(\frac{1 - \frac{\chi_1(v - q) + \chi_2(v - q)^2}{u}}{1 - \frac{\chi_1(v - q) + \chi_2(v - q)^2}{p}} \right)^{r-1} \\ L(u, v) &:= \left[\frac{\tilde{H}(u, v)}{H_x(p, q)(u - p)} \right]^{-\beta} \end{aligned}$$

Thus, showing that the integrands in Lemma 1 are asymptotically equivalent is the same as showing that K and L are asymptotically equal to 1. We will show this for u in γ_1 , and for the parts of γ_2 and γ_3 sufficiently close to the critical point.

Lemma 2. Assume $v \in \mathcal{C}_y$ with $|\theta| \leq r^{-\frac{2}{5}}$. Also, assume that either $u \in \gamma_1$, or that $u \in \gamma_2 \cup \gamma_3$ with $u = p + \frac{\omega t}{r}$ and $t \leq r^{\frac{3}{10}}$. Then, the following holds uniformly as $r, s \rightarrow \infty$ with $\lambda = \frac{r+O(1)}{s}$:

$$K(u, v) = 1 + o(1)$$

Proof. We pull aside the numerator of $K(u, v)$:

$$\begin{aligned} 1 - \frac{\chi_1(v - q) + \chi_2(v - q)^2}{u} &= 1 - \frac{\chi_1(v - q) + \chi_2(v - q)^2}{p - (p - u)} \\ &= 1 - \frac{\chi_1(v - q) + \chi_2(v - q)^2}{p} \cdot \frac{1}{1 - \left(1 - \frac{u}{p}\right)} \end{aligned}$$

For $u \in \gamma_1$, $|u - p| = \frac{1}{r}$. Thus, we have $\left(1 - \frac{u}{p}\right) = O(r^{-1})$, and $\left|1 - \frac{u}{p}\right| < 1$ for r sufficiently large. Hence, we can expand $\frac{1}{1 - \left(1 - \frac{u}{p}\right)}$ as a uniformly convergent geometric series for all $u \in \gamma_1$.

This yields the following:

$$1 - \frac{\chi_1(v - q) + \chi_2(v - q)^2}{u} = 1 - \frac{\chi_1(v - q) + \chi_2(v - q)^2}{p} \left[1 + \left(1 - \frac{u}{p}\right) + \left(1 - \frac{u}{p}\right)^2 + \dots \right] \quad (3.4)$$

Now, we can replace the numerator in the base of K by the expression in (3.4) to obtain the following:

$$\frac{1 - \frac{\chi_1(v-q) + \chi_2(v-q)^2}{u}}{1 - \frac{\chi_1(v-q) + \chi_2(v-q)^2}{p}} = 1 - \frac{\frac{\chi_1(v-q) + \chi_2(v-q)^2}{p}}{1 - \frac{\chi_1(v-q) + \chi_2(v-q)^2}{p}} \left[\left(1 - \frac{u}{p}\right) + O\left(1 - \frac{u}{p}\right)^2 \right] \quad (3.5)$$

Equation (3.5) holds uniformly for $|\theta| \leq r^{-\frac{2}{5}}$ and u in the region of the lemma, as $r \rightarrow \infty$. Between γ_1 and the regions of γ_2 and γ_3 described in the lemma, $\left(1 - \frac{u}{p}\right) = O\left(r^{-\frac{7}{10}}\right)$. Also, from (3.3), $|v - q| = O\left(r^{-\frac{2}{5}}\right)$. Plugging these facts into (3.5) yields the following:

$$\frac{1 - \frac{\chi_1(v-q) + \chi_2(v-q)^2}{u}}{1 - \frac{\chi_1(v-q) + \chi_2(v-q)^2}{p}} = 1 + O\left(r^{-\frac{11}{10}}\right)$$

We replace the base of K with this new expression:

$$K(u, v) = \left(1 + O\left(r^{-\frac{7}{5}}\right)\right)^{-r-1} = e^{(-r-1)\ln\left(1 + O\left(r^{-\frac{11}{10}}\right)\right)}$$

The Taylor series for the natural logarithm gives us the following estimate:

$$\ln\left(1 + O\left(r^{-\frac{11}{10}}\right)\right) = O\left(r^{-\frac{11}{10}}\right)$$

Thus, we may complete the lemma:

$$K(u, v) = e^{(-r-1) \cdot O\left(r^{-\frac{11}{10}}\right)} = e^{O\left(r^{-\frac{1}{10}}\right)} = 1 + o(1)$$

□

Next, we prove the corresponding statement for $L(u, v)$ on γ_1 or the parts of γ_2 and γ_3 sufficiently close to p .

Lemma 3. Assume $v \in \mathcal{C}_y$ with $|\theta| \leq r^{-\frac{2}{5}}$. Also, assume either that $u \in \gamma_1$, or that $u \in \gamma_2 \cup \gamma_3$ with $u = p + \frac{\omega t}{r}$ and $t \leq r^{\frac{3}{10}}$. Then, the following holds uniformly as $r, s \rightarrow \infty$ with $\lambda = \frac{r+O(1)}{s}$:

$$L(u, v) = 1 + o(1)$$

Proof. Recall that $\tilde{H}(u, v)$ has a particularly nice power series:

$$\tilde{H}(u, v) = \sum_{m, n \geq 0} d_{mn} (u - p)^m (v - q)^n$$

In this series, we have the restrictions, $d_{00} = d_{01} = d_{02} = 0$. Hence, we can express \tilde{H} in the following manner:

$$\tilde{H} = d_{10}(u - p) + f(u, v) + g(u, v) + h(u, v) \quad (3.6)$$

Here, we define f, g , and h by $f(u, v) = O(u-p)^2, g(u, v) = O((u-p)(v-q))$, and $h(u, v) = O(v-q)^3$, each uniformly as (u, v) approaches (p, q) . Also, we note from (3.2) above that $d_{10} = H_x(p, q)$.

We now plug (3.6) into the definition of L :

$$\begin{aligned} L(u, v) &:= \left[\frac{\tilde{H}(u, v)}{H_x(p, q)(u - p)} \right]^{-\beta} \\ &= \left[1 + \frac{f + g + h}{H_x(p, q)(u - p)} \right]^{-\beta} \end{aligned} \quad (3.7)$$

In the region described in this Lemma, we have the restrictions, $\frac{1}{r} \leq |u - p| \leq r^{-\frac{7}{10}}$, and $|v - q| = O\left(r^{-\frac{2}{5}}\right)$. Thus, we obtain the following expressions:

$$\begin{aligned} \frac{f}{H_x(p, q)(u - p)} &= O(u - p) = O\left(r^{-\frac{7}{10}}\right) \\ \frac{g}{H_x(p, q)(u - p)} &= O(v - q) = O\left(r^{-\frac{2}{5}}\right) \\ \frac{h}{H_x(p, q)(u - p)} &= O\left(\frac{(v - q)^3}{u - p}\right) = O\left(r \cdot \left(r^{-\frac{2}{5}}\right)^3\right) = O\left(r^{-\frac{1}{5}}\right) \end{aligned}$$

Each of these statements holds uniformly over the region in the lemma as $r \rightarrow \infty$. Plugging these into (3.7) above yields the desired result:

$$L(u, v) = \left[1 + O\left(r^{-\frac{1}{5}}\right) \right]^{-\beta} = 1 + o(1)$$

□

This completes the proof that our integrand is essentially a product integrand near the critical point. It remains to show that the contributions away from the critical point are negligible.

3.4.2 $(v - q)$ or $(u - p)$ is Big

Here, we justify that the away from the critical point, the contribution to the integral decays exponentially faster than the contribution near the critical point.

Lemma 4. Let $\bar{\mathcal{C}}(p, q)$ represent the portion of $\mathcal{C}(p, q)$ where at least one of the following conditions holds: $|\theta| > r^{-\frac{2}{5}}$ or $|u - q| \geq r^{-\frac{7}{10}}$. Then, the following holds uniformly as $r, s \rightarrow \infty$ with $\lambda = \frac{r+O(1)}{s}$:

$$\begin{aligned} \left(\frac{1}{2\pi i}\right)^2 \iint_{\bar{\mathcal{C}}(p,q)} \tilde{H}(u, v)^{-\beta} (u - \chi_1(v - q) - \chi_2(v - q)^2)^{-r-1} v^{-s-1} du dv \\ = O\left(p^{-r} q^{-s} r^{|\beta|} e^{-\frac{d}{2} r^{\frac{1}{5}}}\right) \end{aligned}$$

Proof. We bound the terms of the integrand separately. First, recall the nice power series, $\tilde{H}(u, v) = \sum_{m,n \geq 0} d_{mn} (u - p)^m (v - q)^n$, with the relations, $d_{00} = d_{01} = d_{02} = 0$ and $\tilde{H}(p + \kappa(v), v) = 0$. Define \bar{u} by $\bar{u} = u - p - \tilde{\kappa}(v)$ and \bar{v} by $\bar{v} = v - q$. $\tilde{H}(p + \kappa(v), v)$ can be represented as follows:

$$0 = \tilde{H}(p + \kappa(v), v) = d_{10}\kappa(v) + d_{11}\kappa(v)\bar{v} + d_{20}\kappa(v)^2 + d_{03}\bar{v}^3 + \dots$$

With this in mind, we expand the power series of $\tilde{H}(p + \tilde{\kappa}(v) + \bar{u}, v)$ to extract $\tilde{H}(p + \kappa(v), v)$:

$$\begin{aligned} \tilde{H}(p + \tilde{\kappa}(v) + \bar{u}, v) &= d_{10}(\kappa(v) + [\tilde{\kappa} - \kappa](v) + \bar{u}) + d_{20}(\kappa(v) + [\tilde{\kappa} - \kappa](v) + \bar{u})^2 \\ &\quad + d_{11}(\kappa(v) + [\tilde{\kappa} - \kappa](v) + \bar{u}) \cdot (\bar{v}) + d_{03}\bar{v}^3 + \dots \\ &= \tilde{H}(p + \kappa(v), v) + d_{10}([\tilde{\kappa} - \kappa](v) + \bar{u}) \\ &\quad + O([\tilde{\kappa} - \kappa](v))^2 + O(\bar{u})^2 + O([\tilde{\kappa} - \kappa](v)\bar{u}) \\ &\quad + O(\kappa(v)[\tilde{\kappa} - \kappa](v)) + O(\kappa(v)\bar{u}) \\ &\quad + O([\tilde{\kappa} - \kappa](v)\bar{v}) + O(\bar{u}\bar{v}) \end{aligned}$$

To see that these seven big-O terms cover every possible term after the d_{03} term in the expansion of \tilde{H} , notice that every term past the d_{03} term must have a power of $(\kappa(v) + [\tilde{\kappa} - \kappa](v) + \bar{u})$ of at least two, or a power of \bar{v} of at least one and a power of $(\kappa(v) + [\tilde{\kappa} - \kappa](v) + \bar{u})$ of at least one. Listing all of the terms of $(\kappa(v) + [\tilde{\kappa} - \kappa](v) + \bar{u})^2$ and $(\kappa(v) + [\tilde{\kappa} - \kappa](v) + \bar{u}) \cdot \bar{v}$ and omitting the overlapping terms from $\tilde{H}(p + \kappa(v), v)$ gives the seven big-O terms above.

Recall that $[\tilde{\kappa} - \kappa](v) = O(\bar{v}^3)$ and $\kappa(v) = O(\bar{v}^3)$. For $|\theta| \leq r^{-\frac{7}{20}}$, $\bar{v} = O\left(r^{-\frac{7}{20}}\right)$ by (3.3), so that $[\tilde{\kappa} - \kappa](v) = O\left(r^{-\frac{21}{20}}\right)$. However, for $|\theta| \geq r^{-\frac{7}{20}}$, $\tilde{\kappa}$ is exactly κ . Thus, $\tilde{\kappa} - \kappa = O\left(r^{-\frac{21}{20}}\right)$ for

all $|\theta| \leq \theta_y$. Additionally, $|\bar{u}| \geq \frac{1}{r}$ on all parts of $\bar{\mathcal{C}}$. Therefore, for ϵ_x, ϵ_y , and θ_x sufficiently small, all terms in the expansion of \tilde{H} are negligible except $d_{10}\bar{u}$. Since $|\bar{u}| \geq \frac{1}{r}$, we have the following bound uniformly on $\bar{\mathcal{C}}$ when $\beta > 0$:

$$\tilde{H}^{-\beta} = O(r^\beta) \quad (3.8)$$

When $\beta < 0$, notice that H is bounded on compact sets, so $H^{-\beta}$ is bounded by a constant. Thus, regardless of the sign of β , we have the following bound:

$$\tilde{H}^{-\beta} = O(r^{|\beta|})$$

Now, we turn to the remaining part of the integrand. Using the relation, $s = \frac{r}{\lambda} + O(1)$ as $r, s \rightarrow \infty$, we break down v^{-s-1} :

$$v^{-s-1} = v^{-1+O(1)}v^{-\frac{r}{\lambda}}$$

Now, we take a factor of p^{-r} out of $(u - \chi_q(v - q) - \chi_2(v - q)^2)^{-r}$ and a factor of $q^{-\frac{r}{\lambda}}$ out of $v^{-\frac{r}{\lambda}}$ to obtain the following decomposition:

$$\begin{aligned} & (u - \chi_1(v - q) - \chi_2(v - q)^2)^{-r-1} v^{-s-1} \\ &= p^{-r} q^{-\frac{r}{\lambda}} (u - \chi_1(v - q) - \chi_2(v - q)^2)^{-1} v^{-1+O(1)} e^{-r\varphi(u,v)} \end{aligned} \quad (3.9)$$

Here, φ is defined by $\varphi(u, v) = \ln\left(\frac{1}{p}[u - \chi_1(v - q) - \chi_2(v - q)^2]\right) + \lambda^{-1} \ln\left[\frac{v}{q}\right]$. We can expand φ as a bivariate power series and obtain the following:

$$\varphi(u, v) = \frac{1}{p}(u - p) + \frac{M}{2}(v - q)^2 + O((u - p)(v - q)) + O(u - p)^2 + O(v - q)^3 \quad (3.10)$$

This equation holds uniformly as (u, v) approaches (p, q) . M has the following definition:

$$M := \left. \frac{\partial^2 \varphi}{\partial v^2} \right|_{(u,v)=(p,q)} = -\frac{2\chi_2}{p} - \frac{\chi_1^2}{p^2} - \frac{1}{\lambda q^2}$$

Rewriting $\varphi(u, v)$ in terms of $\tilde{\kappa}, \bar{u}$, and \bar{v} gives the following:

$$\begin{aligned} \varphi(u, v) &= \varphi(p + \tilde{\kappa}(v) + \bar{u}, q + c\bar{v}) \\ &= \frac{1}{p}(\tilde{\kappa}(v) + \bar{u}) + \frac{M}{2}(\bar{v})^2 + O((\tilde{\kappa}(v) + \bar{u})(\bar{v})) + O(\tilde{\kappa}(v) + \bar{u})^2 + O(\bar{v})^3 \\ &= \frac{1}{p}\bar{u} + \frac{M}{2}(\bar{v})^2 + O(\bar{u}\bar{v}) + O(\bar{u})^2 + O(\bar{v})^3 \end{aligned}$$

The last line holds uniformly as $\bar{u}, \bar{v} \rightarrow 0$, and we used the fact that $\tilde{\kappa}(v) = O(\bar{v})^3$ here. Using that $\bar{v} = qi\theta + O(\theta)^2$, we rewrite $\varphi(u, v)$ one more time:

$$\varphi(u, v) = \frac{1}{p}\bar{u} - \frac{q^2M}{2}\theta^2 + O(\theta\bar{u}) + O(\bar{u})^2 + O(\theta)^3$$

From here, our goal is to bound $e^{-r\varphi}$ in magnitude. To do so, we will investigate the real part of φ . Let $d = \operatorname{Re}\left(-\frac{q^2M}{2}\right)$, which is a strictly positive number by assumption. We break into cases now.

Case 1: When $u \in \gamma_1$ and $|\theta| \geq r^{-\frac{2}{5}}$, we have that $|\bar{u}| = \frac{1}{r}$, which is much smaller than θ^2 .

$$\operatorname{Re}(\varphi(u, v)) = \operatorname{Re}\left(-\frac{q^2M}{2}\theta^2 + o(\theta)^2\right) \geq \frac{dr^{-\frac{4}{5}}}{2}$$

The above inequality holds for r sufficiently large and for ϵ_x and θ_y small enough. Thus, we obtain the following for r sufficiently large:

$$\left|e^{-r\varphi(u, v)}\right| \leq e^{-\frac{d}{2}r^{\frac{1}{5}}}$$

Case 2: Consider the case where $u \in \gamma_2$ or γ_3 and $|\bar{u}| \leq r^{-\frac{7}{10}}$, but $|\theta| \geq r^{-\frac{2}{5}}$. (This case only applies when $|\theta|$ is sufficiently small, since γ_2 and γ_3 are not part of the contour if $|v - q|$ is too large.) Here, we have that $\frac{1}{p}\bar{u} = \frac{1}{p}(u - p - \kappa(v))$ is a strictly positive real number, and it dominates all \bar{u} terms in $\varphi(u, v)$. Thus, \bar{u} only contributes to the decay, and our bound is even more favorable than in Case 1. The following holds for sufficiently large r and sufficiently small ϵ_x and θ_y :

$$\operatorname{Re}(\varphi(u, v)) = \operatorname{Re}\left(-\frac{q^2M}{2}\theta^2 + o(\theta)^2\right) \geq \frac{dr^{-\frac{4}{5}}}{2}$$

So, once again, we obtain this bound:

$$\left|e^{-r\varphi(u, v)}\right| \leq e^{-\frac{d}{2}r^{\frac{1}{5}}}$$

Case 3: Consider the case where $u \in \gamma_2$ or γ_3 and $|\bar{u}| \geq r^{-\frac{3}{10}}$. (Once again, this case is only relevant when $|\theta|$ is small enough for γ_2 and γ_3 to be part of the contour.) For sufficiently small ϵ_x and θ_y , the $O(\bar{u}\theta)$ term is dominated by the \bar{u} term. The remaining θ terms are dominated

by the θ^2 term, so these θ terms can only increase the real part of φ . Thus, the real part of φ is at least half the $\frac{1}{p}\bar{u}$ term, and we have the following for r sufficiently large:

$$\operatorname{Re}(\varphi(u, v)) \geq \frac{1}{2|p|} r^{-\frac{3}{10}}$$

Plugging this into the exponential yields the following:

$$\left| e^{-r\varphi(u, v)} \right| \leq e^{-\frac{1}{2|p|} r^{\frac{7}{10}}}$$

Case 4: Now, consider the case where $u \in \gamma_4$ or γ_5 and $|\theta| \leq \frac{1}{2}\epsilon_y$. Then, $|u - \tilde{\kappa}(v)| = |p| + \epsilon_x$. Thus, we have the following information about the leading term of φ :

$$\begin{aligned} \left| \frac{1}{p}\bar{u} \right| &= \left| \frac{1}{p} \right| |u - p - \tilde{\kappa}(v)| \\ &\geq \left| \frac{1}{p} \right| [|u - \tilde{\kappa}(v)| - |p|] \\ &= \frac{\epsilon_x}{|p|} \end{aligned} \tag{3.11}$$

Also, for θ_x sufficiently small (depending on ϵ_x and $|p|$), the following holds:

$$|\arg(u - p - \tilde{\kappa}(v)) - \arg(p)| \leq \frac{\pi}{3} \tag{3.12}$$

Equivalently:

$$\left| \arg\left(\frac{u}{p} - 1 - \frac{\tilde{\kappa}(v)}{p}\right) \right| \leq \frac{\pi}{3}$$

This statement should be clear graphically: let $\alpha = \arg\left(\frac{u}{p} - 1 - \frac{\tilde{\kappa}(v)}{p}\right)$, and consider Figure 3.4. Clearly, as θ_x tends to zero, α approaches zero as well. Combining (3.11) and (3.12), we have the following:

$$\operatorname{Re}\left[\frac{1}{p}\bar{u}\right] \geq \frac{\epsilon_x}{|p|} \cos(\arg(u - p - \tilde{\kappa}(v)) - \arg(p)) \geq \frac{1}{2} \frac{\epsilon_x}{|p|}$$

Just like in Case 3, in the expansion of φ , the $O(\bar{u}\theta)$ term is dominated by the \bar{u} term, and the remaining θ terms are dominated by the θ^2 term, which only adds to the real part of φ .

Therefore, we can bound the remaining real part in (3.13) as follows:

$$\begin{aligned} \operatorname{Re} \left[\frac{u - \tilde{\kappa}(v)}{p} \right] &\geq \left| \frac{u - \tilde{\kappa}(v)}{p} \right| \cos \theta_x \\ &\geq \left(1 + \frac{\delta}{|p|} \right) \cos \theta_x \end{aligned}$$

In the last line, we used the fact that on γ_4 and γ_5 , $|u - \tilde{\kappa}(v)| \geq |p| + \delta$. For θ_x sufficiently small, dependent on ϵ_y, δ , and $|p|$, we can force this condition (assuming $\delta < |p|$):

$$\cos \theta_x \geq 1 - \frac{\frac{\delta}{2}}{|p| + \delta} = \frac{|p| + \frac{\delta}{2}}{|p| + \delta}$$

Rearranging, this gives us the following:

$$\left(1 + \frac{\delta}{|p|} \right) \cos \theta_x \geq 1 + \frac{\delta}{2|p|}$$

Plugging this into (3.13) yields:

$$\operatorname{Re} \left(\frac{\bar{u}}{p} \right) \geq \frac{\delta}{2|p|}$$

The θ^2 term in the expansion of φ again only contributes to the real part of φ , giving us:

$$\operatorname{Re}(\varphi(u, v)) \geq \frac{\delta}{2|p|}$$

Thus, we obtain exponential decay:

$$\left| e^{-r\varphi(u, v)} \right| \leq e^{-\frac{\delta}{4|p|}r}$$

In every case, we have the following bound for $\epsilon_x, \theta_x, \theta_y$, and δ sufficiently small and r sufficiently large:

$$\left| e^{-r\varphi(u, v)} \right| \leq e^{-\frac{\delta}{2}r^{\frac{1}{5}}} \tag{3.14}$$

Finally, notice that for $\epsilon_x, \epsilon_y, \theta_x$, and δ sufficiently small,

$$\left| (u - \chi_1(v - q) - \chi_2(v - q)^2)^{-1} v^{-1+O(1)} \right| \leq 2 \left| p^{-1} q^{-1+O(1)} \right| \tag{3.15}$$

Plugging (3.14) and (3.15) back into (3.9) gives the following:

$$\left| (u - \chi_1(v - q) - \chi_2(v - q)^2)^{-r-1} v^{-s-1} \right| \leq 2p^{-r-1} q^{-s-1+O(1)} e^{-\frac{\delta}{2}r^{\frac{1}{5}}} \tag{3.16}$$

Recognizing that the entire domain of integration has size bounded by a constant, we combine (3.8) and (3.16) to get the desired result:

$$\left(\frac{1}{2\pi i}\right)^2 \iint_{\tilde{\mathcal{C}}(p,q)} \tilde{H}(u,v)^{-\beta} (u - \chi_1(v-q) - \chi_2(v-q)^2)^{-r-1} v^{-s-1} du dv = O\left(p^{-r} q^{-s} r^{|\beta|} e^{-\frac{d}{2} r^{\frac{1}{5}}}\right)$$

□

Now we prove the corresponding statement for the product integral.

Lemma 5. Let \mathcal{C}_ℓ^* represent the portion of \mathcal{C}_ℓ where $|u - q| \geq r^{-\frac{7}{10}}$. Then, the following holds uniformly as $r, s \rightarrow \infty$ with $\lim_{r,s \rightarrow \infty} \frac{r}{s} = \lambda$:

$$\begin{aligned} \left(\frac{1}{2\pi i}\right)^2 \iint_{\mathcal{C}_\ell^*(p,q)} [H_x(p,q) \cdot (u-p)]^{-\beta} u^{-r-1} v^{-s-1} \left[1 - \frac{\chi_1(v-q) + \chi_2(v-q)^2}{p}\right]^{-r-1} du dv \\ = O\left(p^{-r} q^{-s} r^{|\beta|} e^{-\frac{d}{2} r^{\frac{1}{5}}}\right) \end{aligned}$$

Proof. This proof is a simplified version of the proof for Lemma 4.

First, notice that $|u - p| \geq \frac{1}{r}$ on \mathcal{C}_ℓ^* . Hence, we have the following bound:

$$[H_x(p,q) \cdot (u-p)]^{-\beta} = O\left(r^{|\beta|}\right) \quad (3.17)$$

We manipulate the rest of the integrand:

$$\begin{aligned} u^{-r-1} v^{-s-1} \left[1 - \frac{\chi_1(v-q) + \chi_2(v-q)^2}{p}\right]^{-r-1} \\ = p^{-r} q^{-\frac{r}{\lambda}} u^{-1} v^{-1+O(1)} \left[1 - \frac{\chi_1(v-q) + \chi_2(v-q)^2}{p}\right]^{-1} e^{-r\varphi^*(u,v)} \quad (3.18) \end{aligned}$$

Here, $\varphi^*(u,v)$ is defined by $\varphi^*(u,v) = \ln\left(\frac{u}{p}\right) + \lambda^{-1} \ln\left(\frac{v}{q}\right) + \ln\left[1 - \frac{\chi_1(v-q) + \chi_2(v-q)^2}{p}\right]$. Expanding $\varphi^*(u,v)$ yields a power series very similar to the series for $\varphi(u,v)$:

$$\varphi^*(u,v) = \frac{1}{p}(u-p) + \frac{M}{2}(v-q)^2 + O((u-p)(v-q)) + O(u-p)^2 + O(v-q)^3$$

This equation holds uniformly as (u,v) approaches (p,q) , and M has the same definition as in Lemma 4. Notice that the first few terms of the power series of φ^* match the terms of the power series of φ , (3.10), from Lemma 3.17. $\tilde{\kappa}(v)$ is not present in \mathcal{C}_ℓ^* , but we can substitute 0 for $\tilde{\kappa}(v)$

in the computations leading up to (3.14) in Lemma 4 (excluding the irrelevant cases where $v - q$ is large), which shows that (3.14) still holds here:

$$\left| e^{-r\varphi^*(u,v)} \right| \leq e^{-\frac{d}{2}r^{\frac{1}{5}}} \quad (3.19)$$

Finally, for $\epsilon_x, \theta_x, \theta_y$, and δ sufficiently small, we have the following bound:

$$\left| u^{-1}v^{-1+O(1)} \left[1 - \frac{\chi_1(v-q) + \chi_2(v-q)^2}{p} \right] - 1 \right| \leq 2 \left| p^{-1}q^{-1+O(1)} \right| \quad (3.20)$$

Since the domain of integration has size bounded by a constant, combining (3.17), (3.19), and (3.20) finishes the proof. □

We have nearly completed the proof of Lemma 1. However, it is not yet clear that the bounds we have found away from the critical point are small compared to the value of the whole integral. It turns out that the exponential term in these bounds, $e^{-\frac{d}{2}r^{\frac{1}{5}}}$, will ensure that these bounds are small compared to the integral overall. To show this, it remains to evaluate the asymptotic contribution of the product integral, which will simultaneously show that the contributions to the integral away from the critical point are negligible.

3.5 Proof of Theorem

Lemma 1 has reduced our work to computing the following:

$$\left(\frac{1}{2\pi i} \right)^2 \iint_{\mathcal{C}_\ell(p,q)} [H_x(p,q) \cdot (u-p)]^{-\beta} u^{-r-1} v^{-s-1} \left[1 - \frac{\chi_1(v-q) + \chi_2(v-q)^2}{p} \right]^{-r-1} du dv$$

We break it up into a product integral:

$$\left(\frac{1}{2\pi i} \right)^2 \left(\int_U [H_x(p,q) \cdot (u-p)]^{-\beta} u^{-r-1} du \right) \left(\int_V v^{-s-1} \left[1 - \frac{\chi_1(v-q) + \chi_2(v-q)^2}{p} \right]^{-r-1} dv \right) \quad (3.21)$$

Above, U is the u -projection of the contour, \mathcal{C}_ℓ , which resembles the x contour in Figure 4.8, but with $G(y) = 0$. V is likewise the v -projection, which is the set, $\{v : v = qe^{i\theta}, |\theta| \leq r^{-\frac{2}{5}}\}$. We analyze each of these two integrals separately.

Lemma 6. The following holds uniformly as $r, s \rightarrow \infty$ with $\lambda = \frac{r+O(1)}{s}$:

$$\int_U [H_x(p, q) \cdot (u - p)]^{-\beta} u^{-r-1} du = \frac{2\pi i}{\Gamma(\beta)} r^{\beta-1} p^{-r} \{(-H_x(p, q)p)^{-\beta}\}_P e^{-\beta(2\pi i\omega)} + o(r^{\beta-1} p^{-r})$$

Here, ω is defined to be the signed number of times the curve $H(tp, tq)$ crosses the branch cut in the definition of the function $\{x^{-\beta}\}_P$, as described in the statement of the Theorem.

Proof. The contour U is comprised of the segments γ_i for $1 \leq i \leq 5$ in the case where $|v - q| \leq r^{-\frac{2}{5}}$. The endpoints of the contour, at the beginning of γ_4 and end of γ_5 , both have magnitude $|u| = |p| + \epsilon_x$. We can attach these endpoints to a portion of the circle $\{u : |u| = |p| + \epsilon_x\}$ to form a closed cycle \mathcal{C}_u that wraps around the origin and contains no singularities of $[H_x(p, q) \cdot (u - p)]^{-\beta}$. Because u^{-r-1} is exponentially smaller on the circle $\{u : |u| = |p| + \epsilon_x\}$ than it is near the critical point p , we have:

$$\int_U [H_x(p, q) \cdot (u - p)]^{-\beta} u^{-r-1} du = (1 + o(1)) \int_{\mathcal{C}_u} [H_x(p, q) \cdot (u - p)]^{-\beta} u^{-r-1} du$$

Now, we can use the Cauchy integral formula to evaluate this integral. However, we finally must worry about how the analytic continuation of $H^{-\beta}$ is defined. $H(0, 0)$ is nonzero by assumption, and the values of $H^{-\beta}$ are defined near the origin of \mathbb{C}^2 by the generating function itself. Separately from the analytic continuation of $H^{-\beta}$ that we have used up to this point, we choose a branch of the logarithm with the following properties: the branch must agree with $H^{-\beta}$ on some small neighborhood of the origin, and its branch cut must be a line from the origin that is *not* the line $\ell(t) = -tH_x(p, q)p$ for $t \geq 0$, for any of the critical points (p, q) . Define $\{x^{-\beta}\}_P$ as the value of $x^{-\beta}$ obtained by using this branch of the logarithm.

Consider the curve $H(tp, tq)$ in \mathbb{C} , with $t \in [0, 1)$. This curve may wrap around the origin several times, and in particular, may cross the branch cut described above. Recall the bivariate

power series for $H(x, y)$:

$$H(x, y) = \sum_{m, n \geq 0} h_{mn}(x - p)^m(y - q)^n$$

Plugging in our parameterization yields:

$$\begin{aligned} H(tp, tq) &= h_{10}(tp - p) + h_{01}(tq - q) + \cdots \\ &= -(1 - t)ph_{10} - (1 - t)qh_{01} + O(1 - t)^2 \\ &= (1 - t)(-ph_{10} - qh_{01}) + O(1 - t)^2 \end{aligned}$$

The above equations are true as $t \rightarrow 1$. Recall the following conditions: $H_x(p, q) \neq 0$, and $H_y(p, q) = \frac{p}{\lambda q} H_x(p, q)$. Plugging this into our computations above yields:

$$H(tp, tq) = (1 - t)(-p(1 + \lambda)H_x(p, q)) + O(1 - t)^2$$

Thus, as t tends to 1, the curve $H(tp, tq)$ is essentially linear, with quadratic error. As long as the branch cut chosen above is not the line $\ell(t)$ mentioned above, the curve will only cross the branch cut finitely many times. Let ω be the signed number of times the curve $H(tp, tq)$ crosses the branch cut in the counter-clockwise direction for $t \in [0, 1)$. That is, every time the curve crosses the branch cut in the counter-clockwise direction, add 1 to ω , and every time it crosses in the clockwise direction, subtract 1 from ω . If the curve only touches the branch cut without crossing it, leave ω unchanged.

As t approaches 1, we have shown that H behaves essentially like $H_x(p, q)(u - p)$, and we have traced how the argument changes as we expand the two-dimensional torus towards the critical point. Now, in order to revert the integral over \mathcal{C}_u back to the appropriate coefficient of $H_x(p, q)(u - p)$ by using the Cauchy integral formula, we must follow the image of $H_x(p, q)(u - p)$ from $u = p$ back to the origin $u = 0$. As u follows the line from p to 0, the $H_x(p, q)(u - p)$ will follow the line in \mathbb{C} from 0 to $-pH_x(p, q)$, the point whose power we are trying to determine. Because this straight line is $\ell(t)$, it will not cross the branch cut we chose above. Thus, ω already accounts for the total number of times the branch cut is crossed. Figure 3.5 shows an example of this setup. In this

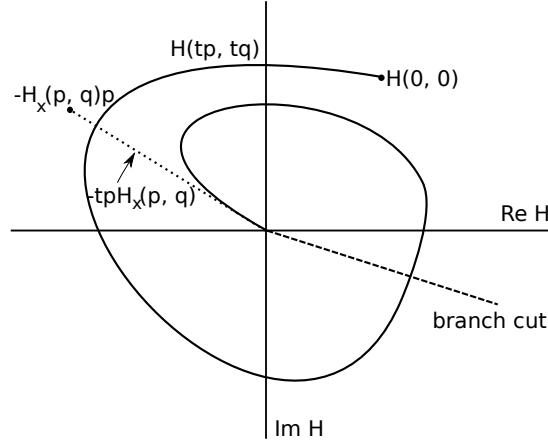


Figure 3.5: An example with $\omega = 1$.

example, $\omega = 1$, because $H(tp, tq)$ crosses the branch cut once in the counter-clockwise direction.

In conclusion, we have the following:

$$\begin{aligned}
 \int_{\mathcal{C}_u} [H_x(p, q) \cdot (u - p)]^{-\beta} u^{-r-1} du &= (1 + o(1)) 2\pi i [u^r] (H_x(p, q) \cdot (u - p))^{-\beta} \\
 &= (1 + o(1)) 2\pi i (H_x(p, q))^r \binom{-\beta}{r} \\
 &\quad \cdot \{(-H_x(p, q)p)^{-\beta-r}\}_P e^{-\beta(2\pi i\omega)} \tag{3.22}
 \end{aligned}$$

From Stirling's approximation, we have the following:

$$\binom{-\beta}{r} \sim \frac{r^{\beta-1}}{\Gamma(\beta)} (-1)^r$$

Additionally, we can separate the integer portion of the power of $-H_x(p, q)p$:

$$\{(-H_x(p, q)p)^{-\beta-r}\}_P = \{(-H_x(p, q)p)^{-\beta}\}_P (-H_x(p, q)p)^{-r}$$

Plugging these two expressions into (3.22) and simplifying yields the result:

$$\int_{\mathcal{C}_u} [H_x(p, q) \cdot (u - p)]^{-\beta} u^{-r-1} du = \frac{2\pi i}{\Gamma(\beta)} r^{\beta-1} p^{-r} \{(-H_x(p, q)p)^{-\beta}\}_P e^{-\beta(2\pi i\omega)} + o(r^{\beta-1} p^{-r})$$

□

We turn our attention to the other integral, and find its asymptotic contribution.

Lemma 7. The following holds uniformly as $r, s \rightarrow \infty$ with $\lambda = \frac{r+O(1)}{s}$:

$$\int_V v^{-s-1} \left[1 - \frac{\chi_1(v-q) + \chi_2(v-q)^2}{p} \right]^{-r-1} dv = iq^{-s} \sqrt{\frac{2\pi}{-q^2 Mr}} + o\left(q^{-s} r^{-\frac{1}{2}}\right)$$

Here, the square root is taken to be the principal root.

Proof. Note that $\lambda = \frac{r+O(1)}{s}$ implies that $s = -\frac{r}{\lambda} + O(1)$. We rewrite the integrand:

$$\begin{aligned} v^{-s-1} \left[1 - \frac{\chi_1(v-q) + \chi_2(v-q)^2}{p} \right]^{-r-1} &= q^{-s-1} \left(\frac{v}{q} \right)^{-s-1} \left[1 - \frac{\chi_1(v-q) + \chi_2(v-q)^2}{p} \right]^{-r-1} \\ &= q^{-s-1} \left(\frac{v}{q} \right)^{O(1)} e^{-r\psi(v)} \end{aligned}$$

In the last line, we define ψ as:

$$\psi(v) := \log \left[1 - \frac{\chi_1(v-q) + \chi_2(v-q)^2}{p} \right] + \frac{1}{\lambda} \log \left(\frac{v}{q} \right)$$

We expand $\psi(v)$ as a Taylor series about $v = q$:

$$\psi(v) = \frac{M}{2}(v-q)^2 + O(v-q)^3$$

Also, since $v = qe^{i\theta}$ and $|\theta| \leq r^{-\frac{2}{5}}$, we have the following:

$$\left(\frac{v}{q} \right)^{O(1)} = 1 + o(1)$$

Plugging these expressions into the integral and rewriting it in terms of θ gives us the following:

$$\begin{aligned} &\int_V v^{-s-1} \left[1 - \frac{\chi_1(v-q) + \chi_2(v-q)^2}{p} \right]^{-r-1} dv \\ &= q^{-s-1} \int_V e^{-r\left[\frac{M}{2}(v-q)^2 + O(v-q)^3\right]} (1 + o(1)) dv \\ &= q^{-s-1} [1 + o(1)] \int_{-r^{-\frac{2}{5}}}^{r^{\frac{2}{5}}} e^{-r\left[-\frac{q^2 M}{2}\theta^2 + O(\theta)^3\right]} iq e^{i\theta} d\theta \\ &= iq^{-s} [1 + o(1)] \int_{-r^{-\frac{2}{5}}}^{r^{\frac{2}{5}}} e^{-r\left[-\frac{q^2 M}{2}\theta^2 + O(\theta)^3\right]} e^{i\theta} d\theta \\ &= iq^{-s} [1 + o(1)] \int_{-r^{-\frac{2}{5}}}^{r^{\frac{2}{5}}} e^{-r\left[-\frac{q^2 M}{2}\theta^2\right]} e^{i\theta} d\theta \quad (3.23) \end{aligned}$$

The last line is true because $O(\theta)^3 = O\left(r^{-\frac{6}{5}}\right)$ implies that $e^{-rO(\theta)^3} = 1 + o(1)$. The remaining integral is nearly a Fourier-Laplace integral, but it has a shrinking domain of integration. We justify that this can be replaced by a domain of integration of constant size. Specifically, we aim to show that for some $\epsilon > 0$ small enough, the following holds:

$$\int_{-r^{-\frac{2}{5}}}^{r^{\frac{2}{5}}} e^{-r\left[-\frac{q^2 M}{2}\theta^2\right]} e^{i\theta} d\theta = \int_{-\epsilon}^{\epsilon} e^{-r\left[-\frac{q^2 M}{2}\theta^2\right]} e^{i\theta} d\theta + O\left(e^{-\frac{d}{2}r^{\frac{1}{5}}}\right) \quad (3.24)$$

To see this, notice that if $|\theta| \geq r^{-\frac{2}{5}}$, then we have:

$$\operatorname{Re}\left(-\frac{q^2 M}{2}\theta^2\right) \geq \frac{d}{2}r^{-\frac{4}{5}}$$

This implies the following:

$$\left|e^{-r\left[-\frac{q^2 M}{2}\theta^2\right]}\right| \leq e^{-\frac{d}{2}r^{\frac{1}{5}}}$$

In turn, this implies:

$$\int_{r^{-\frac{2}{5}} \leq |\theta| \leq \epsilon} e^{-r\left[-\frac{q^2 M}{2}\theta^2\right]} e^{i\theta} d\theta = O\left(e^{-\frac{d}{2}r^{\frac{1}{5}}}\right)$$

This completes the proof of (3.24). To analyze the remaining integral, we use the standard saddle point approximation, which is proved in Theorem 4.1.1 in [PW13]. The amplitude $A(\theta) = e^{i\theta}$ and the phase $\phi(\theta) = -\frac{q^2 M}{2}\theta^2$ are both analytic functions near $\theta = 0$, and $\operatorname{Re}(\phi) \geq 0$ on the interval $[-\epsilon, \epsilon]$, with equality only at $\theta = 0$. Thus, we have:

$$\int_{-\epsilon}^{\epsilon} e^{-r\left[-\frac{q^2 M}{2}\theta^2\right]} e^{i\theta} d\theta = (1 + o(1))A(0)\sqrt{\frac{2\pi}{\phi''(0)r}}e^{-r\phi(0)} = (1 + o(1))\sqrt{\frac{2\pi}{-q^2 Mr}} \quad (3.25)$$

In the above expression, the square root is the principal root. Plugging (3.25) into the remaining integral in (3.23) finishes the proof. \square

Plugging the results of Lemma 6 and Lemma 3.23 into (3.21) gives us the final result:

$$\begin{aligned} & \left(\frac{1}{2\pi i}\right)^2 \int_U [H_x(p, q) \cdot (u - p)]^{-\beta} u^{-r-1} du \int_V v^{-s-1} \left[1 - \frac{\chi_1}{p}(v - q) - \frac{\chi_2}{p}(v - q)^2\right]^{-r-1} dv \\ & = [1 + o(1)] \frac{r^{\beta-\frac{3}{2}} p^{-r} q^{-s} \{(-H_x(p, q)p)^{-\beta}\}_P e^{-\beta(2\pi i\omega)}}{\Gamma(\beta)\sqrt{-2\pi q^2 M}} \end{aligned}$$

3.6 Corollary

Unfortunately, for general H , the formula in the Theorem becomes quite messy, as we must find how many times the image of H wraps around the origin along the path connecting $(0, 0)$ to each critical point (p, q) . Additionally, the sign of the square root in the formula can cause headaches. Luckily, in the case where H has only real coefficients and there is a single smooth strictly minimal critical point, we can simplify the formula.

Corollary 3.6.1. *Let H be an analytic function with a single smooth strictly minimal critical point (p, q) , where p and q are real and positive. Let H have only real coefficients in its power series expansion about the origin. Assume $H(0, 0) > 0$, and consider $H^{-\beta}$ for $\beta \in \mathbb{R}$ with $\beta \notin \mathbb{Z}_{\leq 0}$. Also, define $H^{-\beta}$ here with the standard branch chosen along the negative real axis, so that $H(0, 0)^{-\beta} > 0$. Let $\lambda = \frac{r+O(1)}{s}$ as $r, s \rightarrow \infty$. Define the following quantities:*

$$\begin{aligned}\chi_1 &= \frac{H_y(p, q)}{H_x(p, q)} = \frac{p}{\lambda q} \\ \chi_2 &= \frac{1}{2H_x} (\chi_1^2 H_{xx} - 2\chi_1 H_{xy} + H_{yy}) \Big|_{(x,y)=(p,q)} \\ M &= -\frac{2\chi_2}{p} - \frac{\chi_1^2}{p^2} - \frac{1}{\lambda q^2}\end{aligned}$$

Assume that $H_x(p, q)$ and M are nonzero. Then, the following expression holds as $r, s \rightarrow \infty$:

$$[x^r y^s] H(x, y)^{-\beta} \sim \frac{r^{\beta-\frac{3}{2}} p^{-r} q^{-s} (-H_x(p, q)p)^{-\beta}}{\Gamma(\beta) \sqrt{-2\pi q^2 M}}$$

In the above expression, $-H_x(p, q)p$ will be a positive real number, and $(-H_x(p, q)p)^{-\beta}$ will also be a positive real number. Additionally, $-2\pi q^2 M$ is positive, so the positive square root is taken.

Proof. Since H has real coefficients and p and q are positive real numbers, we must have that $-H_x(p, q)p$ is real. The line $H(tp, tq)$ for $0 \leq t \leq 1$ is real and can't pass through the origin since (p, q) is minimal. Also, the line from 0 to $-H_x(p, q)p$ is real, and it approximates $H(tp, tq)$ for t near 1, as described in Section 3.5 and Figure 3.5 above. This would mean that $-H_x(p, q)p$ is in

fact positive. Additionally, the line $H(tp, tq)$ cannot wrap around the origin, which forces $\omega = 0$ in the statement of the original Theorem. As a result, $\{(-H_x(p, q)p)^{-\beta}\}_P$ is positive. With this term positive, the only other term with an unknown sign is $\sqrt{-2\pi q^2 M}$. However, knowing that $-2\pi q^2 M$ is real, in order for the coefficients of $H^{-\beta}$ to be real at all, $-2\pi q^2 M$ must be negative. Thus, $\sqrt{-2\pi q^2 M}$ is always positive (since the principal root is taken), which forces the whole formula to be positive always. \square

3.7 Example

We will look at the coefficients $x^r y^s$ of the following bivariate generating function:

$$F(x, y) = \frac{1 - x(1 + y)}{\sqrt{1 - 2x(1 + y) - x^2(1 - y)^2}}$$

This example comes from a problem of Ron Graham and Fan Chung Graham (through personal correspondence), motivated by their research generalizing the cover polynomials of digraphs. Because each y term is attached to an x of equal or greater power, the power series expansion of F will have no terms where the power of y is larger than the power of x . Thus, we will look at the asymptotics only the case where $\mu := \lambda^{-1} = \frac{s}{r} \in (0, 1)$. (We switch to μ so that the range of possible directions is bounded.)

To begin, we find the critical points of the denominator, $H(x, y) = 1 - 2x(1 + y) - x^2(1 - y)^2$.

We will use a Gröbner basis to compute these points in terms of μ . In Maple, after importing the `Groebner` package, the command is as follows:

$$\mathbf{gb} := \mathbf{Basis}([\mathbf{H}, \mathbf{y} * \mathbf{diff}(\mathbf{H}, \mathbf{y}) - \mathbf{mu} * \mathbf{x} * \mathbf{diff}(\mathbf{H}, \mathbf{x})], \mathbf{plex}(\mathbf{x}, \mathbf{y})); \quad (3.26)$$

This command returns a basis of polynomials which vanishes collectively at exactly the same points that the original polynomials H and $yH_y - \mu x H_x$ vanished. However, by specifying the pure lexicographical order with $x > y$, the Gröbner basis will attempt to eliminate y from the first

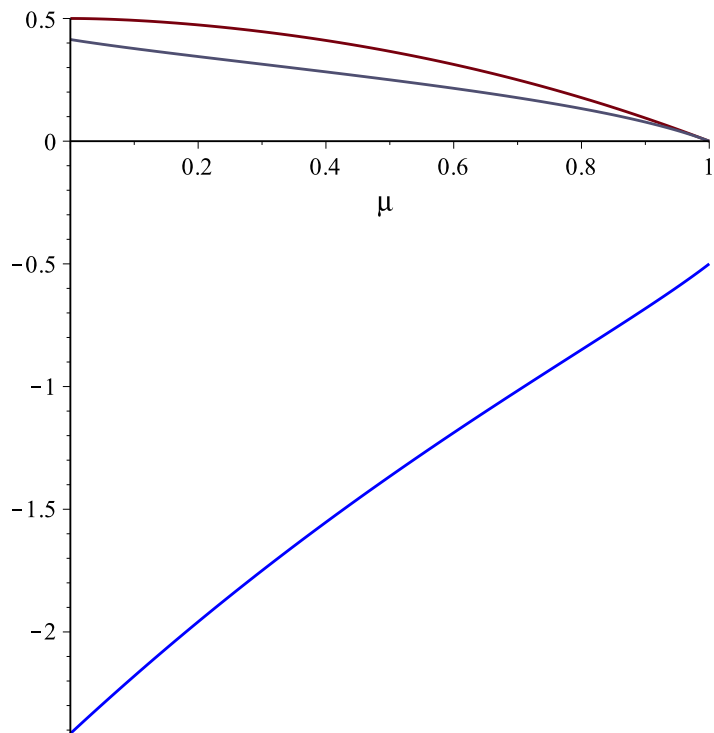


Figure 3.6: The three x critical solution curves of H , in terms of $\mu = \frac{s}{r}$.

polynomial in the basis. Here, the first polynomial in the basis is as follows:

$$1 - 2\mu + \mu^2 + (-4 - 2\mu^2 + 6\mu)x + 2x^3 + (2\mu^2 - 4\mu + 3)x^2 \quad (3.27)$$

Because this is a degree 3 polynomial in x , we can solve for the three values of x explicitly in terms of μ . A graph of these solutions for $\mu \in (0, 1)$ is shown in Figure 3.6.

Once the x solutions are found, they can be plugged into the second basis element of the Gröbner basis to compute the corresponding y solutions in terms of μ . We must check that all of these critical points are smooth. To do so, we find the following Gröbner basis:

$$\text{Basis}([\mathbf{H}, \mathbf{y} * \text{diff}(\mathbf{H}, \mathbf{y}) - \mu * \mathbf{x} * \text{diff}(\mathbf{H}, \mathbf{x}), \text{diff}(\mathbf{H}, \mathbf{x})], \text{plex}(\mathbf{x}, \mathbf{y}))$$

This command returns `[1]`, which means that there is never a time when all of these terms vanish.

Thus, H_x is never zero at any of the critical points, so they are all smooth critical points. Similarly,

we can check if $x = 0$ or $y = 0$ for any of the critical point pairs by computing the following Gröbner bases in Maple:

$$\text{gbx} := \text{Basis}([\text{H}, \text{y} * (\text{diff}(\text{H}, \text{y})) - \text{mu} * \text{x} * \text{diff}(\text{H}, \text{x}), \text{x}], \text{plex}(\text{y}, \text{x}, \text{mu})) \quad (3.28)$$

$$\text{gby} := \text{Basis}([\text{H}, \text{y} * (\text{diff}(\text{H}, \text{y})) - \text{mu} * \text{x} * \text{diff}(\text{H}, \text{x}), \text{y}], \text{plex}(\text{y}, \text{x}, \text{mu})) \quad (3.29)$$

The first returns the trivial basis, $[1]$, while the second has the first basis element, μ , which implies that $\mu = 0$ is the only time when y can be zero. Thus, the solutions are never zero for $\mu \in (0, 1)$.

Showing that the curvature, M , is nonzero becomes a little more complicated. We can use a Gröbner basis to compute M in terms of μ by using the command,

$$\begin{aligned} \text{gb} := \text{Basis}([\text{H}, \text{y} * \text{Hy} - \text{mu} * \text{x} * \text{Hx}, \text{Hx} * \text{chi1} - \text{Hy}, 2 * \text{Hx} * \text{chi2} - \text{chi1}^2 * \text{Hxx} + \\ 2 * \text{chi1} * \text{Hxy} - \text{Hyy}, 2 * \text{chi2} * \text{y}^2 * \text{x} + \text{chi1}^2 * \text{y}^2 + \text{mu} * \text{x}^2], \text{plex}(\text{chi1}, \text{chi2}, \text{y}, \text{x}, \text{mu})) \end{aligned}$$

Here, the first two equations restrict the x and y values to the critical points. The third equation defines χ_1 implicitly, while the fourth equation defines χ_2 implicitly, and the fifth equation sets $M = 0$. The first basis element of the resulting Gröbner basis is:

$$-\mu - 10\mu^2 + 12\mu^3 - 4\mu^4 + 2\mu^5$$

It is easy to verify via Sturm sequences that none of the five solutions to this equation occur in $\mu \in (0, 1)$.

It remains to check the critical points for minimality. Before showing that an individual critical point is minimal, we compare the height function $h = \log|x| + \mu \log|y|$ for each of the three critical point pairs (x_i, y_i) . The critical point pair with the smallest height value will be our candidate for the minimal critical point. We plot the three height curves in Figure 3.7, and see that one of the solutions has a height below the other two. To prove that one of the solutions is indeed below the other two, we begin by showing that all three solution pairs are real. Looking at the polynomial

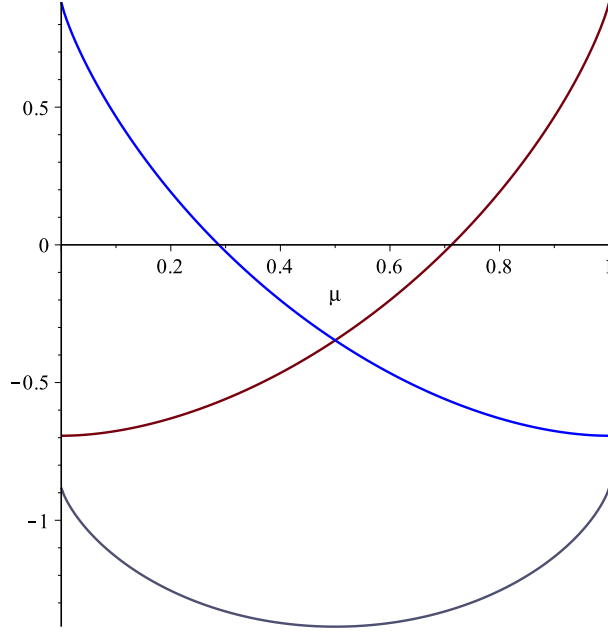


Figure 3.7: The magnitude of the three critical point solutions (x, y) , in terms of $\mu = \frac{s}{r}$.

the x -solutions satisfy, (3.27), we compute the discriminant of this cubic equation:

$$\begin{aligned} -\frac{1}{216} + \frac{43}{72}\mu^4 - 1/2\mu^3 + \frac{5}{27}\mu^6 - \frac{5}{12}\mu^5 + \frac{1}{108}\mu^8 - 1/18\mu^7 + \frac{23}{108}\mu^2 - 1/36\mu \\ = \frac{1}{216} (2\mu^4 - 4\mu^3 + 12\mu^2 - 10\mu - 1)(\mu - 1)^4 \end{aligned}$$

The roots of a cubic polynomial are real if the discriminant is negative. Of course, the $(\mu - 1)^4$ term is positive, so we must show that the remaining factor is negative. We notice that

$$2\mu^4 - 4\mu^3 + 12\mu^2 - 10\mu = 2\mu(\mu - 1)(\mu^2 - \mu + 5)$$

On $\mu \in (0, 1)$, $\mu > 0$, $\mu - 1 < 0$, and $\mu^2 - \mu + 5 > 4$ since it has a global minimum of 4.75 at $\mu = 1/2$. Thus, overall, $2\mu^4 - 4\mu^3 + 12\mu^2 - 10\mu < 0$ and $2\mu^4 - 4\mu^3 + 12\mu^2 - 10\mu - 1 < 0$. So, indeed, the discriminant is negative and all three x solutions are real. The second element of the Gröbner basis gb from (3.26) is:

$$4 - \mu^3 + 5\mu^2 - 8\mu + (-8 + 2\mu^3 + 13\mu - 8\mu^2)x + (-4 + 2\mu)x^2 + (\mu^3 - 3\mu^2 + 3\mu - 1)y$$

Setting this to zero and solving for y shows that if x is real, then so is y . Thus, each critical point pair is real. Knowing that x_i and y_i are never zero from the Gröbner bases `gbx` and `gby` (equations (3.28) and (3.29)), we can conclude that for each of the three solution curves $(x_i(\mu), y_i(\mu))$, each component x_i and y_i is always positive or always negative for all $\mu \in (0, 1)$. By testing a specific value of μ on each of the three curves, we find that one solution has $x > 0, y < 0$, another has $x < 0, y < 0$, and the last has $x > 0, y > 0$. Thus, the height function h can be written $h = \log(\pm x) + \mu \log(\pm y)$, where the signs depend on which solution curve we are examining. Taking the derivative of h with respect to μ yields:

$$\frac{\partial h}{\partial \mu} = \frac{1}{x} \frac{dx}{d\mu} + \frac{\mu}{y} \frac{dy}{d\mu} + \log(\pm y)$$

Again, the sign in front of y depends on which solution curve we are examining. After solving for x and y explicitly, the following is easily verified:

$$\frac{1}{x} \frac{dx}{d\mu} + \frac{\mu}{y} \frac{dy}{d\mu} = 0$$

Thus, we can simplify the derivative of h :

$$\frac{\partial h}{\partial \mu} = \log(\pm y)$$

So, the critical points occur where $y = \pm 1$. We can find which μ correspond to these y by using two more Gröbner bases:

$$\text{gby1} := \text{Basis}([\mathbb{H}, y * (\text{diff}(\mathbb{H}, y)) - \mu * x * \text{diff}(\mathbb{H}, x), y - 1], \text{plex}(y, x, \mu))$$

$$\text{gby2} := \text{Basis}([\mathbb{H}, y * (\text{diff}(\mathbb{H}, y)) - \mu * x * \text{diff}(\mathbb{H}, x), y + 1], \text{plex}(y, x, \mu))$$

`gby1` has first basis element $2\mu - 1$, while `gby2` has first basis element $-\mu + \mu^2$. Thus, the potential locations of critical points of h between all three solution curves are at $\mu = 0, 1/2$, and 1 . Plugging in these values of μ into the three different solution curves shows that the solution curve where $x > 0$ and $y > 0$ has a global maximum less than the global minimum of the other two solution curves for $\mu \in (0, 1)$. (Two of the solution curves are undefined at $\mu = 1$, so we take limits as

$\mu \rightarrow \infty$ instead.) Thus, this is the candidate for the curve of critical points which contributes to the asymptotics.

However, it is still difficult to verify rigorously that this whole curve consists of minimal critical points. Without knowing this, it is unknown whether these critical points actually contribute to the asymptotics. One approach is presented in [DeV11], where DeVries presents an algorithm for showing that a given critical point must contribute to the asymptotics of the coefficients. The idea behind the algorithm is as follows: at a critical point (x_0, y_0) , we can compute the degree of degeneracy, k , of the height function, $h = \log|x| + \mu \log|y|$. If $\mathcal{V}^{>c}$ is the subset of \mathcal{V}_H where the height function h is greater than c , then for any sufficiently small neighborhood U of (x_0, y_0) , $U \cap \mathcal{V}^{>h(x_0, y_0)}$ has k connected components. For each connected component A , consider any strictly-ascending path in \mathcal{V}_H starting at (x_0, y_0) , staying in A , and approaching infinity. The x or y coordinate of this path must tend towards 0 in order for the path to remain in \mathcal{V}_H . If there is at least one component where the path tends towards $x = 0$ and at least one component where the path tends towards $y = 0$, then the critical point must contribute to the asymptotics of the coefficients because it creates a topological obstruction to expanding the contour in the Cauchy integral formula. The details of these computations for this example will appear in the published version of this thesis.

To see how well the formula works, we look at the example where $\mu = \frac{1}{2}$. Using the x and y solutions from the Gröbner bases above, we have that the critical point is at $(x, y) = (\frac{1}{4}, 1)$. From here, we can compute the following:

$$\begin{aligned} \chi_1 &= \frac{1}{8} \\ \chi_2 &= -\frac{3}{64} \\ H_x\left(\frac{1}{4}, 1\right) &= -4 \\ M &= -\frac{3}{8} \end{aligned}$$

Thus, from the Corollary above (with $\beta = \frac{1}{2}$), we have that as $r, s \rightarrow \infty$ with $2 = \frac{r+O(1)}{s}$ as

$r, s \rightarrow \infty$,

$$[x^r y^s] H(x, y) \sim \frac{r^{-1} \left(\frac{1}{4}\right)^{-r}}{\Gamma\left(\frac{1}{2}\right) \sqrt{\frac{3\pi}{4}}} = \frac{2 \cdot 4^r}{r\pi\sqrt{3}}$$

If the numerator of F was a monomial $ax^m y^n$, it would simply shift the terms in the series of F by m in the x variable and n in the y variable, and multiply all the coefficients by a . We can break up the numerator of F linearly and compute these shifts separately. Equivalently, to account for the fact that the numerator $G(x, y) := 1 - x(1 + y)$ is not a monomial, we multiply our approximation above by G evaluated at the critical point. In this case, since $G\left(\frac{1}{4}, 1\right) = \frac{1}{2}$, the final approximation is:

$$[x^r y^s] F(x, y) \sim \frac{4^r}{r\pi\sqrt{3}}$$

When $r = 70$, this formula gives approximately $3.65924 \cdot 10^{39}$. Taking derivatives of F reveals that the value of $[x^{70} y^{35}] F(x, y)$ is approximately $3.59821 \cdot 10^{39}$. The ratio of these values is 1.017, showing that the approximation is already quite good for $r = 70$.

3.8 Future Research

One obvious extension of these results is to find more terms in the asymptotic expansion of the coefficients of H . This can be accomplished by using the Cauchy integral formula over the same contour as before. However, one must be much more precise about the error terms and the contributions of each part of the contour to the asymptotics in order to find the lower order terms. That makes the computations even more messy than they are currently.

Another potential extension of these results is to more variables. In the two-variable case, the zero set of H was analyzable by a change of variables which was not originally obvious. However, this change of variables allowed H to be approximated by a one-dimensional binomial function. Thus, the challenge in more dimensions is to find an appropriate change of variables that is simple but still reduces H to a one-dimensional binomial.

Not all algebraic singularities come in the form, $H(x, y)^{-\beta}$. Thus, another direction for future

research is the case where H is only known to satisfy a polynomial equation. Here, the critical points can be computed implicitly, but it is harder to be explicit about finding an appropriate contour in the Cauchy integral.

Finally, combining these results with other asymptotic techniques may yield stronger results and more complete asymptotic expansions, too. For example, creative telescoping methods take the generating function in question and find a partial differential equation that the function satisfies. By finding a basis of solutions to this differential equation, one can find complete asymptotic expansions to the coefficients of the generating function. Unfortunately, it is often difficult to find the correct coefficients of the solution to the PDE – this is referred to as the *connection problem*. However, if the leading-term asymptotics of the solution are known, the connection problem can often be solved. Thus, combining these creative telescoping methods with the first-order asymptotics results in this thesis, one may be able to analyze generating functions without too many technical computations.

Chapter 4

Quantum Walks

4.1 Introduction

Random walks have proven to be a useful tool in creating optimized algorithms for many situations. For example, random walks can contribute to algorithms for counting and sampling, and also algorithms which test properties such as the satisfiability of Boolean formulae or graph connectivity [BP07].

Quantum random walks provide the opportunity to expand upon and better these algorithms. The process was first constructed in the 1990's by [ADZ93], with the idea of using such a process for quantum computing. In their 2001 paper, Ambainis et al pointed out that “quantum random walks have the potential to offer new tools for quantum algorithms,” including that they “may yield techniques for analyzing discrete quantum processes [...] more generally.”

Quantum random walks differ from their classical counterparts because they allow for destructive interference between different paths between the same two locations. In particular, quantum walks frequently encounter this interference near the origin. As a result, particles tend to spread much faster in quantum random walks than in classical random walks. Explicitly, at time n , the location of a quantum random walk's particle is typically found at distance $\theta(n)$ from the origin,

while in a classical random walk, the particle is found at distance $\theta(\sqrt{n})$ from the origin.

4.1.1 Preliminaries

For our discrete quantum random walks, we first choose a dimension d for the integer lattice \mathbb{Z}^d around which the particle moves. Next, we need to add a degree of freedom to allow for quantum interference. This extra degree of freedom, called a chirality, is somewhat like the spin of a particle. Each chirality j corresponds to one way a particle can move throughout the walk, defined by a vector $\mathbf{v}^{(j)} \in \mathbb{Z}^d$. For example, in a simple 1-dimensional case, there may be 2 chiralities: one which corresponds to moving one step to the left, and one which corresponds to moving one step to the right. Throughout our models of a walk, the chirality of a particle will describe the last step the particle took. Overall, this gives the state space for the quantum random walk,

$$\Omega := L^2(\mathbb{Z}^d \times \{1, \dots, k\})$$

A Hilbert Basis for Ω is the set of elementary states $\delta_{\mathbf{r},j}$, as \mathbf{r} ranges over \mathbb{Z}^d and $1 \leq j \leq k$; we will also denote $\delta_{\mathbf{r},j}$ simply by (\mathbf{r}, j) .

Next, the walk needs a unitary matrix U to describe how any chirality transforms into the other chiralities during a step of the walk. Although in general U can take complex values, we restrict to the case where U is real for ease of computations. For a k -chirality walk, U will be a $k \times k$ unitary matrix. Let $I \otimes U$ denote the unitary operator on Ω whose value on the elementary state (\mathbf{r}, j) is equal to $\sum_{i=1}^k U_{ij}(\mathbf{r}, i)$. Let T denote the operator whose action on the elementary states is given by $T(\mathbf{r}, j) = (\mathbf{r} + \mathbf{v}^{(j)}, j)$. The QRW operator $\mathcal{S} = \mathcal{S}_{d,k,U,\{\mathbf{v}^{(j)}\}}$ is defined by

$$\mathcal{S} := T \cdot (I \otimes U) . \tag{4.1}$$

More informally, a step of a QRW may be broken down into two parts: first, change the chiralities of the particle by acting on it by U . The nj th entry of U gives a square root of the probability that a particle starting in chirality n changes to chirality j in any given step - so, the

n th column of the matrix describes the distribution of a particle of chirality n after it has taken its next step. For the second part of the step, move the particles according to their new chiralities. It is important to notice that even when we restrict to real values, U matrix will have both positive and negative entries. This is because these values represent amplitudes, which are squared to give probabilities. By allowing negative amplitudes, the particles may interfere with each other throughout the walk. The fact that the matrix is unitary guarantees that the total probability of a particle being anywhere always adds up to 1 after every step.

Therefore, to fully set up any quantum random walk, we need a collection of chiralities, a corresponding unitary matrix, and an initial distribution. The initial distribution simply tells the probability of our particle starting at any location, with any given amplitudes.

Notice that the QRW is translation invariant, meaning that if σ is any translation operator $(\mathbf{r}, j) \mapsto (\mathbf{r} + \mathbf{u}, j)$ then $\mathcal{S} \circ \sigma = \sigma \circ \mathcal{S}$. The n -step operator is \mathcal{S}^n . Using bracket notation, we denote the amplitude for finding the particle in chirality j and location $\mathbf{x} + \mathbf{r}$ after n steps, starting in chirality i and location \mathbf{x} , by

$$a(i, j, n, \mathbf{r}) := \langle (\mathbf{x}, i) | \mathcal{S}^n | (\mathbf{x} + \mathbf{r}, j) \rangle . \tag{4.2}$$

By translation invariance, this quantity is independent of \mathbf{x} . The squared modulus $|a(i, j, n, \mathbf{r})|^2$ is interpreted as the probability of finding the particle in chirality j and location $\mathbf{x} + \mathbf{r}$ after n steps, starting in chirality i and location \mathbf{x} , if a measurement is made. Unlike the classical random walk, the quantum random walk can be measured only at one time without disturbing the process. We may therefore study limit laws for the quantities $a(i, j, n, \mathbf{r})$ but not joint distributions of these.

4.2 Examples

4.2.1 Hadamard QRW

As an example, we look at the classic Hadamard walk, which was defined in [ADZ93] and analyzed in [ABN⁺01] and [CIR03]. The walk has two chiralities, which correspond to staying still and moving one step to the right - and in this special case, we name them accordingly: $\{0, 1\}$. The unitary matrix for the walk is as follows:

$$U = \begin{vmatrix} \frac{1}{\sqrt{2}} & \frac{1}{\sqrt{2}} \\ \frac{1}{\sqrt{2}} & -\frac{1}{\sqrt{2}} \end{vmatrix}$$

In general, we assume that all of our particles start at the origin, because a simple translation could make the starting location a new origin. Therefore, we can choose our starting state to be a particle with amplitude 1 in chirality 1. Then, after one step, the distribution of the particle will be as follows: there is a particle at location 0 with an amplitude of $\frac{1}{\sqrt{2}}$ and a chirality of 0, and there is another particle at location 1 with an amplitude of $-\frac{1}{\sqrt{2}}$ and a chirality of 1.

For the second step, the unitary matrix acts upon each theoretical location of the particle. We will get the following four particles, labelled as [location, amplitude, chirality]:

$$\left. \begin{array}{l} [0, \frac{1}{2}, 0] \\ [1, \frac{1}{2}, 1] \end{array} \right\} \text{ coming from the particle at location 0}$$

$$\left. \begin{array}{l} [1, -\frac{1}{2}, 0] \\ [2, \frac{1}{2}, 1] \end{array} \right\} \text{ coming from the particle at location 1}$$

Notice that the particles at 1 do not yet interfere because they have different chiralities. It is not until the next step of the walk that the particles first interfere: this happens only with the particles at 1, who will necessarily move to the same locations with the same chiralities. The

distribution of the particles $[1, \frac{1}{2}, 1]$ and $[1, -\frac{1}{2}, 0]$ are as follows:

$$\left. \begin{array}{l} [1, \frac{1}{2\sqrt{2}}, 0] \\ [2, -\frac{1}{2\sqrt{2}}, 1] \end{array} \right\} \text{ coming from the particle with chirality 1}$$

$$\left. \begin{array}{l} [1, -\frac{1}{2\sqrt{2}}, 0] \\ [2, -\frac{1}{2\sqrt{2}}, 1] \end{array} \right\} \text{ coming from the particle with chirality 0}$$

So here, the two paths which led to a particle at position 1 will cancel with each other completely, leaving no particle at this location with chirality 0. On the other hand, the particles at location 2 will constructively interfere, giving a particle with amplitude $-\frac{1}{\sqrt{2}}$ and chirality 1 at this location.

As previous works have shown, up to a rapidly oscillating factor due to a phase difference in two summands in the amplitude, the rescaled amplitudes $n^{1/2}a(i, j, n, n\theta)$ converge to a profile $f(\theta)$ supported on the interval $J := \left[\frac{1}{2} - \frac{\sqrt{2}}{4}, \frac{1}{2} + \frac{\sqrt{2}}{4} \right]$. The function f is continuous on the interior of J and blows up like $|\theta - \theta_0|^{-1/2}$ when θ_0 is an endpoint of J . These results are extended in [BP07] to arbitrary unitary matrices. The limiting profiles are all qualitatively similar; a plot for the Hadamard QRW is shown in figure 4.1, with the upper envelope showing what happens when the phases of the summands line up.

4.2.2 Walks with Three or More Chiralities

When the number of chiralities is allowed to exceed two, new phenomena emerge. The possibility of a bound state arises. This means that for some fixed location x , the amplitude $a(i, j, n, x)$ does not go to zero as $n \rightarrow \infty$. This was first shown to occur in [BCA03, IKS05]. From a generating function viewpoint, bound states occur when the denominator Q of the generating function factors. The occurrence of bound states appears to be a non-generic phenomenon.

To investigate these phenomena further, my coworker Rajarshi Das and I wrote codes that would model 1-dimensional quantum random walks with 3 or 4 chiralities, and generalized matrices U and step sizes $\{\mathbf{v}^{(j)}\}$. Many of the walks we modelled are catalogued here:

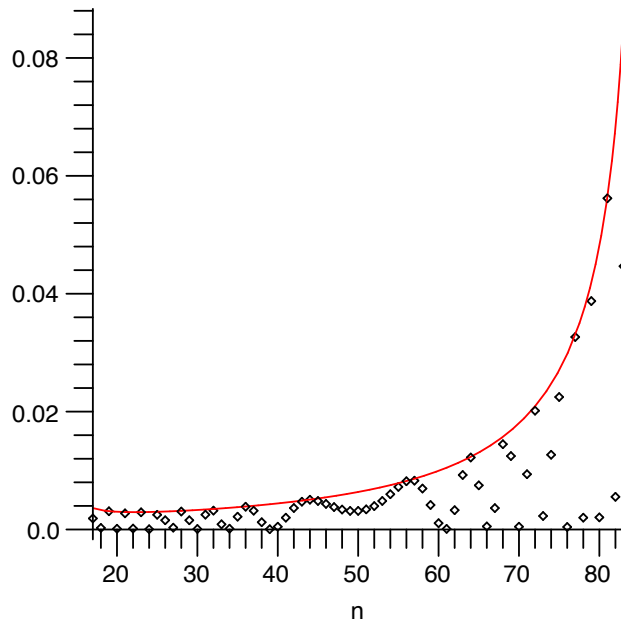


Figure 4.1: probability profile for the one-dimensional Hadamard QRW

http://www.math.upenn.edu/~pemantle/Summer2007/First_Page.html .

The probability profile shown in figure 4.2 is typical of what we found and is the basis for an example running throughout this section. In this example,

$$U = \frac{1}{27} \begin{bmatrix} 17 & 6 & 20 & -2 \\ -20 & 12 & 13 & -12 \\ -2 & -15 & 4 & -22 \\ -6 & -18 & 12 & 15 \end{bmatrix} \quad (4.3)$$

and $\mathbf{v}^{(j)} = -1, 0, 1, 2$ for $j = 1, 2, 3, 4$ respectively. The profile shown in the figure is a plot of $|a(1, 1, 1000, x)|^2$ against x for integers x in the interval $[-1000, 2000]$.

The values were computed exactly by recursion and then plotted. The most obvious new feature is the existence of a number of peaks in the interior of the feasible region. The phase factor is somewhat more chaotic as well, which turns out to be due to a greater number of summands in the amplitude function. Our aim is to use the theory described in Section 2 to establish the locations

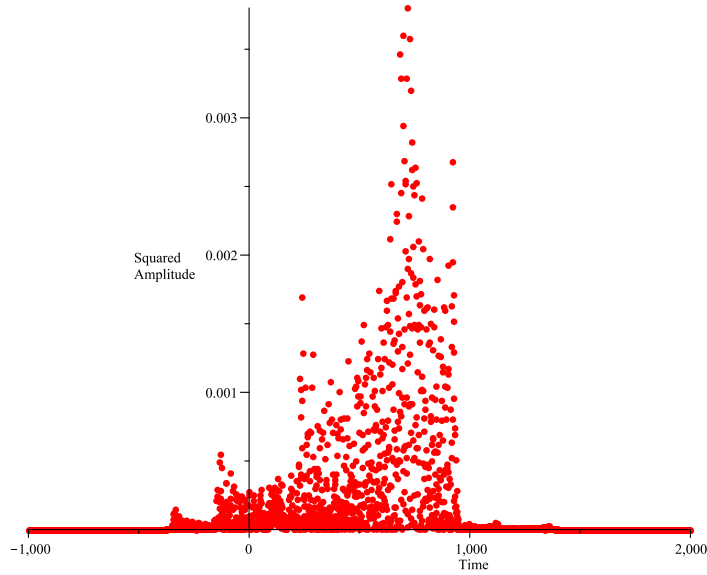


Figure 4.2: probability profile for a four-chirality QRW in one dimension

of these peaks, that is to say, the values of θ for which $n^{1/2}a(i, j, n, x)$ become unbounded for x sufficiently near $n\theta$.

4.2.3 2-dimensional example

We can extend the quantum random walks to two dimensions, adding a component to each chirality to describe the step sizes in the new dimension. For example, we can take a walk with chiralities $\{(1, 0), (-1, 0), (0, 1), (0, -1)\}$, the unitary matrix

$$U := \begin{pmatrix} \frac{51}{305} & -\frac{188}{305} & -\frac{18}{305} & -\frac{234}{305} \\ \frac{116}{305} & -\frac{3}{305} & \frac{282}{305} & \frac{6}{305} \\ -\frac{258}{305} & \frac{54}{305} & \frac{109}{305} & -\frac{108}{305} \\ -\frac{102}{305} & -\frac{234}{305} & \frac{36}{305} & \frac{163}{305} \end{pmatrix},$$

and a starting distribution of the particle with amplitude $\frac{1}{\sqrt{2}}$ in each of the first two chiralities. We plot the graph for 200 steps and get the distribution in Figure ??, where the darker lines represent higher probabilities of being at that location:

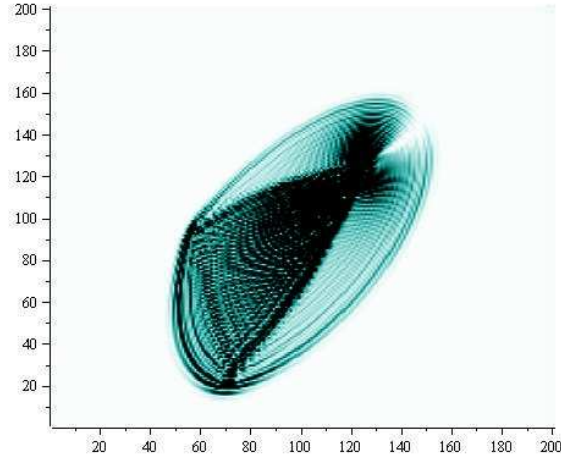


Figure 4.3: The probability distribution of a 2-dimensional QRW after 200 steps.

4.3 Asymptotics

In the following sections, the notation and results mimic those of [BGPP09].

4.3.1 Generating Functions

Quantum random walks show pronounced asymptotes. In particular, for each walk, there are set ratios r/s of location to time where the amplitude of the particle explodes, relative to the amplitudes of nearby locations. Precisely, the peaks are values θ such that $\sqrt{n}a(i, j, n, x)$ becomes unbounded for x sufficiently close to $n\theta$.

We wish to determine exactly where these values of θ are, without approximating them through merely iterating a QRW. The key to analyzing a QRW's graphs is through generating functions. In his book [Wil06], Herbert Wilf describes a generating function as “a clothesline on which we hang up a sequence of numbers for display.” Generating functions encode a sequence of numbers $\{a_n\}_{n=0}^{\infty}$ by encapsulating the information an expression whose power series has the same coefficients $\{a_n\}$.

In what follows, we let \mathbf{x} denote the vector (x_1, \dots, x_d) . Given a lattice QRW, for $1 \leq i, j \leq k$

we may define a power series in $d + 1$ variables via

$$F_{ij}(\mathbf{x}, y) := \sum_{n \geq 0} \sum_{\mathbf{r} \in \mathbb{Z}^d} a(i, j, n, \mathbf{r}) \mathbf{x}^{\mathbf{r}} y^n. \quad (4.4)$$

Here and throughout, $\mathbf{x}^{\mathbf{r}}$ denotes the monomial power $x_1^{r_1} \cdots x_d^{r_d}$. We let \mathbf{F} denote the generating matrix $(F_{ij})_{1 \leq i, j \leq k}$, which is a $k \times k$ matrix with entries in the formal power series ring in $d + 1$ variables. The following result from [BP07] is obtained via a straightforward use of the transfer matrix method.

Lemma 4.3.1 ([BP07, Proposition 3.1]). *Let $M(\mathbf{x})$ denote the $k \times k$ diagonal matrix whose diagonal entries are $\mathbf{x}^{\mathbf{v}^{(1)}}, \dots, \mathbf{x}^{\mathbf{v}^{(k)}}$. Then*

$$\mathbf{F}(\mathbf{x}, y) = (I - yM(\mathbf{x})U)^{-1}. \quad (4.5)$$

Consequently, there are polynomials $P_{ij}(\mathbf{x}, y)$ such that

$$F_{ij} = \frac{P_{ij}}{Q} \quad (4.6)$$

where $Q(\mathbf{x}, y) := \det(I - yM(\mathbf{x})U)$.

Within these generating functions, \mathbf{x} is a placeholder whose power represents the location of a particle, and y is a placeholder whose power represents the number of steps taken by the particle.

Let \mathbf{z} denote the vector (\mathbf{x}, y) and let

$$\mathcal{V} := \{\mathbf{z} \in \mathbb{C}^{d+1} : Q(\mathbf{z}) = 0\}$$

denote the algebraic variety which is the common pole of the generating functions F_{ij} . Let $\mathcal{V}_1 := \mathcal{V} \cap T^{d+1}$ denote the intersection of the singular variety \mathcal{V} with the unit torus $T^{d+1} := \{|x_1| = \cdots = |x_d| = |y| = 1\}$. An important map on \mathcal{V} is the logarithmic Gauss map $\mu : \mathcal{V} \rightarrow \mathbb{C}\mathbb{P}^d$ defined by

$$\mu(\mathbf{z}) := \left(z_1 \frac{\partial Q}{\partial z_1} : \cdots : z_{d+1} \frac{\partial Q}{\partial z_{d+1}} \right). \quad (4.7)$$

The map μ is defined only at points of \mathcal{V} where the gradient ∇Q does not vanish. Here, we will be concerned only with instances of QRW satisfying

$$\nabla Q \text{ vanishes nowhere on } \mathcal{V}_1. \quad (4.8)$$

This condition holds generically.

4.3.2 Previous Results

It is shown in [BBBP10, Proposition 2.1] that the image $\mu[\mathcal{V}_1]$ is contained in the real subspace $\mathbb{R}P^d \subseteq \mathbb{C}P^d$. Also, under the hypothesis (4.8), $\partial Q/\partial y$ cannot vanish on \mathcal{V}_1 , hence we may interpret the range of μ as $\mathbb{R}^d \subseteq \mathbb{R}P^d$ via the identification $(x_1 : \cdots : x_d : y) \leftrightarrow ((x_1/y), \dots, (x_d/y))$. In what follows, we draw heavily on two results from [BBBP10].

Theorem 4.3.2 (shape theorem [BBBP10, Theorem 4.2]). *Assume (4.8) and let $\mathbf{G} \subseteq \mathbb{R}^d$ be the closure of the image of μ on \mathcal{V}_1 . If K is any compact subset of \mathbf{G}^c , then*

$$a(i, j, n, \mathbf{r}) = O(e^{-cn})$$

for some $c = c(K) > 0$, uniformly as \mathbf{r}/n varies over K .

In other words, under ballistic rescaling, the region of non-exponential decay or *feasible region* is contained in \mathbf{G} . The converse, and much more, is provided by the second result, also from the same theorem. For $\mathbf{z} \in \mathcal{V}_1$, let $\kappa(\mathbf{z})$ denote the curvature of the real hypersurface $-i \log \mathcal{V}_1 \subseteq \mathbb{R}^{d+1}$ at the point $\log \mathbf{z}$, where \log is applied to vectors coordinatewise and manifolds pointwise.

Theorem 4.3.3 (asymptotics in the feasible region). *Suppose Q satisfies (4.8). For $\mathbf{r} \in \mathbf{G}$, let $Z(\mathbf{r})$ denote the set $\mu^{-1}(\mathbf{r})$ of pre-images in \mathcal{V}_1 of the projective point \mathbf{r} under μ . If $\kappa(\mathbf{z}) \neq 0$ for all $\mathbf{z} \in Z(\mathbf{r})$, then*

$$a(i, j, n, \mathbf{r}) = n^{-d/2} \left[\sum_{z \in Z(\mathbf{r})} \frac{P_{ij}(\mathbf{z})}{|\nabla_{\log Q}(\mathbf{z})|} |\kappa(\mathbf{z})|^{-1/2} e^{i\omega(\mathbf{r}, n)} \right] + O\left(n^{-(d+1)/2}\right) \quad (4.9)$$

where the argument $\omega(\mathbf{r}, n)$ is given by $-\mathbf{r} \cdot \text{Arg}(\mathbf{z}) + i\pi\tau(\mathbf{z})/4$ and $\tau(\mathbf{z})$ is the index of the quadratic form defining the curvature at the point $(1/i)\log \mathbf{z} \in (1/i)\log \mathcal{V}_1$.

4.4 Results and Conjectures

The results of Section 4.2.2 may be summarized informally in the case of one-dimensional QRW as follows. Provided the quantities ∇Q and κ do not vanish for the points z associated with a direction \mathbf{r} , then the amplitude profile will be a the sum of terms whose phase factors may be somewhat chaotic, but whose magnitudes are proportional to $\kappa^{-1/2}/|\nabla_{\log Q}|$. In practice the magnitude of the amplitude will vary between zero and the sum of the magnitudes of the pieces, depending on the behavior of the phase terms. In the two-chirality case, with only two summands, it is easy to identify the picture with the theoretical result. However, in the multi-chirality case, the empirical results in figure 4.2 are not easily rectified with the theoretical result, firstly because the theoretical result is not trivial to compute, and secondly because the computation appears at first to be at odds with the data. In the remainder of Section 4.2.2, we show how the theoretical computations may be executed in a computer algebra system, and then rectify these with the data in figure 4.2. The first step is to verify some of the hypotheses of Theorems 4.3.2–4.3.3. The second step, reconciling the theory and the data, will be done in Section 4.4.1.

Proposition 4.4.1. *Let $Q(\mathbf{x}, y)$ be the denominator of the generating function for any QRW in any dimension that satisfies the smoothness hypothesis (4.8). Let π be the projection from \mathcal{V}_1 to the d -torus T^d that forgets the last coordinate. Then the following properties hold.*

1. $\partial Q/\partial y$ does not vanish on \mathcal{V}_1 ;
2. \mathcal{V}_1 is a compact d -manifold;
3. $\pi : \mathcal{V}_1 \rightarrow T^d$ is smooth and nonsingular;
4. In fact, \mathcal{V}_1 is homeomorphic to a union of some number s of d -tori, each mapping smoothly to T^d under π and covering T^d some number n_j times for $1 \leq j \leq s$.
5. $\kappa : \mathcal{V}_1 \rightarrow \mathbb{R}$ vanishes exactly when the determinant of the Jacobian of the map μ vanishes.
6. κ vanishes on the boundary $\partial\mu[\mathcal{V}_1]$ of the range of μ .

Proof. The first two conclusions are shown as [BBBP10, Proposition 2.2]. The map π is smooth

on T^{d+1} , hence on \mathcal{V}_1 , and nonsingularity follows from the nonvanishing of the partial derivative with respect to y . The fourth conclusion follows from the classification of compact d -manifolds covering the d -torus. For the fifth conclusion, recall that the Gauss-Kronecker curvature of a real hypersurface is defined as the determinant of the Jacobian of the map taking p to the unit normal at p . We have identified projective space with the slice $z_{d+1} = 1$ rather than with the slice $|\mathbf{z}| = 1$, but these are locally diffeomorphic, so the Jacobian of μ still vanishes exactly when κ vanishes. Finally, if an interior point of a manifold maps to a boundary point of the image of the manifold under a smooth map, then the Jacobian vanishes there, hence the last conclusion follows from the fifth. \square

An empirical fact is that in all of the several dozen quantum random walks we have investigated, the number of components of \mathcal{V}_1 and the degrees of the map π on each component depend on the dimension d and the vector of chiralities, but not on the unitary matrix U .

Conjecture 4.4.1. *If $d, k, \mathbf{v}^{(1)}, \dots, \mathbf{v}^{(k)}$ are fixed and U varies over unitary matrices, then the number of components of \mathcal{V} and the degrees of the map π on each component are constant, except for a set of matrices of positive co-dimension.*

Remark. *The unitary group is connected, so if the conjecture fails then a transition occurs at which \mathcal{V}_1 is not smooth. We know that this happens, resulting in a bound state [IKS05], however in the three-chirality case, the degeneracy does not seem to mark a transition in the topology of \mathcal{V}_1 .*

Specializing to one dimension, the manifold \mathcal{V}_1 is a union of topological circles. The map $\mu : \mathcal{V}_1 \rightarrow \mathbb{R}$ is evidently smooth, so it maps \mathcal{V}_1 to a union of intervals. In all catalogued cases, in fact the range of μ is an interval, so we have the following open question:

Question 4.4.2. *Is it possible for the image of μ to be disconnected?*

Because μ smoothly maps a union of circles to the real line, the Jacobian of the map μ must vanish at least twice on each circle. Let \mathcal{W} denote the set of $\mathbf{z} \in \mathcal{V}_1$ for which $\kappa(\mathbf{z}) = 0$. The

cardinality of \mathcal{W} is not an invariant (compare, for example, the example in Section 4.4.1 with the first 4-chirality example on the web archive). This has the following interesting consequence. Again, because the unitary group \mathcal{U}_k is connected, by interpolation there must be some U for which there is a double degeneracy in the Jacobian of μ . This means that the Taylor series for $\log y$ on \mathcal{V}_1 as a function of $\log x$ is missing not only its quadratic term but its cubic term as well. In a scaling window of size $n^{1/2}$ near the peaks, it is shown in [BP07] that the amplitudes are asymptotic to an Airy function. However, with a double degeneracy, the same method shows a quartic-Airy limit instead of the usual cubic-Airy limit. This may be the first combinatorial example of such a limit and will be discussed in forthcoming work.

Let $W = \{\mathbf{w}^{(0)}, \dots, \mathbf{w}^{(t)}\}$ be a set of vectors in \mathbb{R}^n . Say that W is rationally degenerate if the set of t -tuples $(\mathbf{r} \cdot (\mathbf{w} - \mathbf{w}^{(0)}))_{\mathbf{w} \in W}$ is not dense in $(\mathbb{R} \bmod 2\pi)^t$ as \mathbf{r} varies over \mathbb{Z}^n . Generic t -tuples are rationally nondegenerate because degeneracy requires a number of linear relations to hold over the $2\pi\mathbb{Q}$. If W is rationally nondegenerate, then the distribution on t -tuples $(\mathbf{r} \cdot (\mathbf{w} - \mathbf{w}^{(0)}))_{\mathbf{w} \in W}$ when \mathbf{r} is distributed uniformly over any cube of side M in \mathbb{Z}^d converges weakly to the uniform distribution on $(\mathbb{Z} \bmod 2\pi)^t$. Let $\chi(\alpha_1, \dots, \alpha_t)$ denote the distribution of the square modulus of the sum of t complex numbers chosen independently at random with moduli $\alpha_1, \dots, \alpha_t$ and arguments uniform on $[-\pi, \pi]$. The following result now follows from the above discussion, Theorems 4.3.2 and 4.3.3, and Proposition 4.4.1.

Proposition 4.4.3. *For any one-dimensional QRW, let $Q, Z(\mathbf{r})$ and κ be as above. Let J be the image of \mathcal{V}_1 under μ . Let \mathbf{r} be any point of J such that $\kappa(\mathbf{z}) \neq 0$ for all $\mathbf{z} \in Z(\mathbf{r})$ and $W := (1/i) \log Z(\mathbf{r})$ is rationally nondegenerate. Then for any $\epsilon > 0$ there exists an M such that if $\mathbf{r}(n)$ is a sequence of integer vectors with $\mathbf{r}^{(n)}/n \rightarrow \mathbf{r}$, the empirical distribution of n^d times the squared moduli of the amplitudes*

$$\{a(i, j, n, \mathbf{r}(n) + \xi) : \xi \in \{0, \dots, M-1\}^{d+1}\}$$

is within ϵ of the distribution $\chi(\alpha_1, \dots, \alpha_t)$ where $t = |Z(\mathbf{r})|$, $\{\mathbf{z}^{(j)}\}$ enumerates $Z(\mathbf{r})$, and $\alpha_j =$

$|P_{ij}(\mathbf{z}^{(j)})\kappa(\mathbf{z}^{(j)})^{-1/2}|$. If $\mathbf{r} \notin \bar{J}$, then the empirical distribution converges to a point mass at zero.

Remark. Rational nondegeneracy becomes more difficult to check when the size of $Z(\mathbf{r})$ increases, which happens when the number of chiralities increases. If one weakens the conclusion to convergence to some nondegenerate distribution with support in $I := [0, \sum |P_{ij}(\mathbf{z})^2\kappa(\mathbf{z})^{-1}|]$, then one needs only that not all components of all differences $\log \mathbf{z} - \log \mathbf{z}'$ are rational, for $\mathbf{z}, \mathbf{z}' \in Z(\mathbf{r})$. For the purpose of qualitatively explaining the plots, this is good enough, though the upper envelope may be strictly less than the upper endpoint of I (and the lower envelope may be strictly greater than zero) if there is rational degeneracy.

Comparing to figure 4.2, we see that J appears to be a proper subinterval of $[-1, 2]$, that there appears to be up to seven peaks which are local maxima of the probability profile. These include the endpoints of J (cf. the last conclusion of Proposition 4.4.1) as well as several interior points, which we now understand to be places where the map μ folds back on itself. We now turn our attention to corroborating our understanding of the picture by computing the number and locations of the peaks.

4.4.1 Computations

Much of our computation is carried out symbolically in Maple. Symbolic computation is significantly faster when the entries of U are rational, than when they are, say, quadratic algebraic numbers. Also, Maple sometimes incorrectly simplifies or fails to simplify expressions involving radicals. It is easy to generate quadratically algebraic orthogonal or unitary matrices via the Gram-Schmidt procedure. For rational matrices, however, we turn to a result we found in [LO91].

Proposition 4.4.4. *The map $S \mapsto (I + S)(I - S)^{-1}$ takes the skew symmetric matrices over a field to the orthogonal matrices over the same field. To generate unitary matrices instead, use skew-hermitian matrices S .*

The map in the proposition is rational, so choosing S to be rational, we obtain orthogonal

matrices with rational entries. In our running example,

$$S = \begin{bmatrix} 0 & -3 & -1 & 3 \\ 3 & 0 & 1 & -2 \\ 1 & -1 & 0 & 2 \\ -3 & 2 & -2 & 0 \end{bmatrix},$$

leading to the matrix U of equation (4.3).

The example shows amplitudes for the transition from chirality 1 to chirality 1, so we need the polynomials P_{11} and Q :

$$\begin{aligned} P_{11}(x, y) &= (27x - 15yx^3 - 4yx + 12y^2x^3 - 12y + 4y^2x^2 + 9y^2 - 17y^3x^2)x \\ Q(x, y) &= -17y^3x^2 + 9y^2 + 27x - 12y + 12y^2x^3 + 8y^2x^2 - 15yx^3 - 4y^3x^3 \\ &\quad - 15y^3x + 12y^2x - 4yx - 17yx^2 + 9y^2x^4 - 12y^3x^4 + 27y^4x^3. \end{aligned}$$

The curvature is proportional to the quantity

$$(-xQ_x - yQ_y)xQ_xyQ_y - x^2y^2(Q_y^2Q_{xx} + Q_x^2Q_{xy} - 2Q_xQ_yQ_{xy}),$$

where subscripts denote partial derivatives. Evaluating this leads to xy times a polynomial $K(x, y)$ that is about half a page in Maple 11. The command

```
Basis([Q, K] , plex (y, x));
```

leads to a Gröbner basis, the first element of which is an elimination polynomial $p(x)$, vanishing at precisely those x -values for which there is a pair $(x, y) \in \mathcal{V}$ for which $\kappa(x, y) = 0$. We may also verify that Q is smooth by computing that the ideal generated by $[Q, Q_x, Q_y]$ has the trivial basis, [1].

To pass to the subset of roots of $p(x)$ that are on the unit circle, one trick is as follows. If $z = x + 1/x$ then x is on the unit circle if and only if z is in the real interval $[-2, 2]$. The polynomial defining z is the elimination polynomial $q(z)$ for the basis $[p, 1 - zx + x^2]$. Applying Maple's built-in

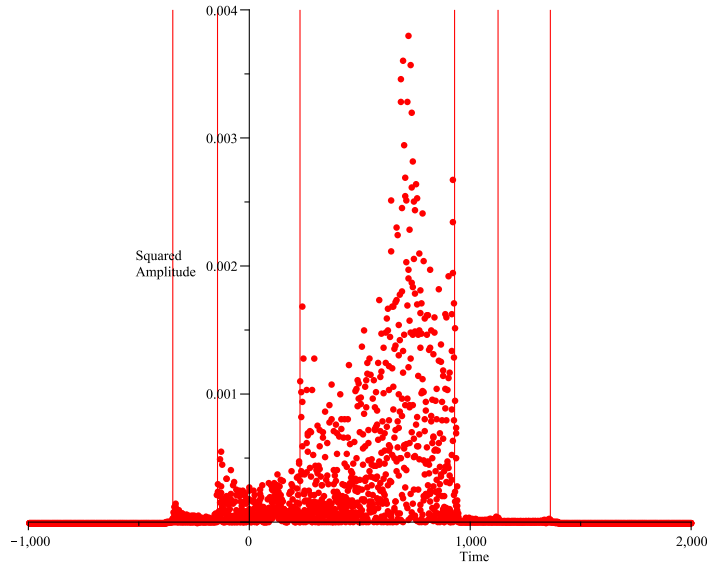


Figure 4.4: probability profile with peaks drawn as vertical lines

Sturm sequence evaluator to q shows symbolically that there are six roots of z in $[-2, 2]$. This leads to six conjugate pairs of x values. The second Gröbner basis element is a polynomial linear in y , so each x value has precisely one corresponding y value. The y value for \bar{x} is the conjugate of the y value for x , and the function μ takes the same value at both points of a conjugate pair. Evaluating the μ function at all six places leads to floating point expressions approximately equal to

$$1.362766, 1.126013, 0.929248, 0.229537, -0.143835, -0.346306.$$

Drawing vertical lines corresponding to these six peak locations leads to figure 4.4.

Surprisingly, the largest peak appearing in the data plot appears to be missing from the set of analytically computed peak directions. Simultaneously, some of the analytically computed peaks appear quite small and it seems implausible that the probability profile blows up there. Indeed, this had us puzzled for quite a while. In order to doublecheck our work, we plotted y against x , resulting in the plot in figure 4.5a, which should be interpreted as having periodic boundary conditions because x and y range over a circle. This shows \mathcal{V}_1 to be the union of two circles, each

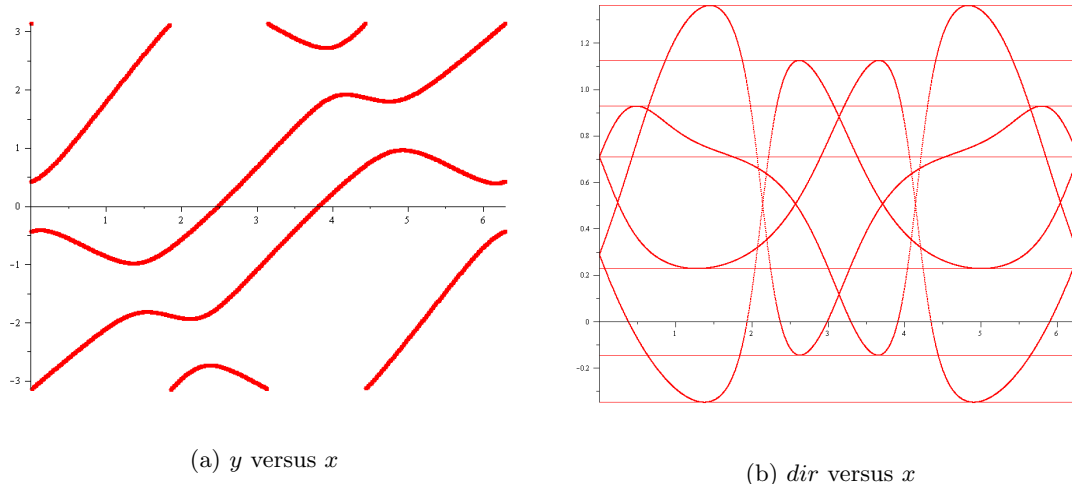


Figure 4.5: Two interleaved circles and their images under the Gauss map.

embedded in T^2 so that the projection π onto x has degree 2. (Note: the projection onto y has degree 1, and the homology class of the embedded circle is $(2, -1)$ in the basis generated by the x and y axes.) We also plotted μ against x . To facilitate computation, we used Gröbner bases to eliminate y from Q and $xQ_x - \mu yQ_y$, enabling us to plot solutions to a single polynomial. The resulting plot is shown in figure 4.5b.

The last figure shows nicely how peaks occur at values where the map μ backtracks. The explanation of the appearance of the extra peak at $\mu \approx 0.7$ becomes clear if we compare plots at $n = 1,000$ and $n = 10,000$.

At first glance, it looks as if the extra peak is still quite prominent, but in fact it has lowered with respect to the others. To be precise, the false peak has gone down by a factor of 10, from 0.004 to 0.0004, because its probabilities scaled as n^{-1} . The width of the peak also remained the same, indicating convergence to a finite probability profile. The real peaks, however, have gone down by factors of $10^{2/3}$, as is shown to occur in the Airy scaling windows near directions \mathbf{r} where $\kappa(\mathbf{z}) = 0$ for some $\mathbf{z} \in Z(\mathbf{r})$. When the plot is vertically scaled so that the highest peak occurs at the same height in each picture, the width above half the maximum has shrunk somewhat, as must occur in an Airy scaling window, which has width \sqrt{n} . The location of the false peak is marked by

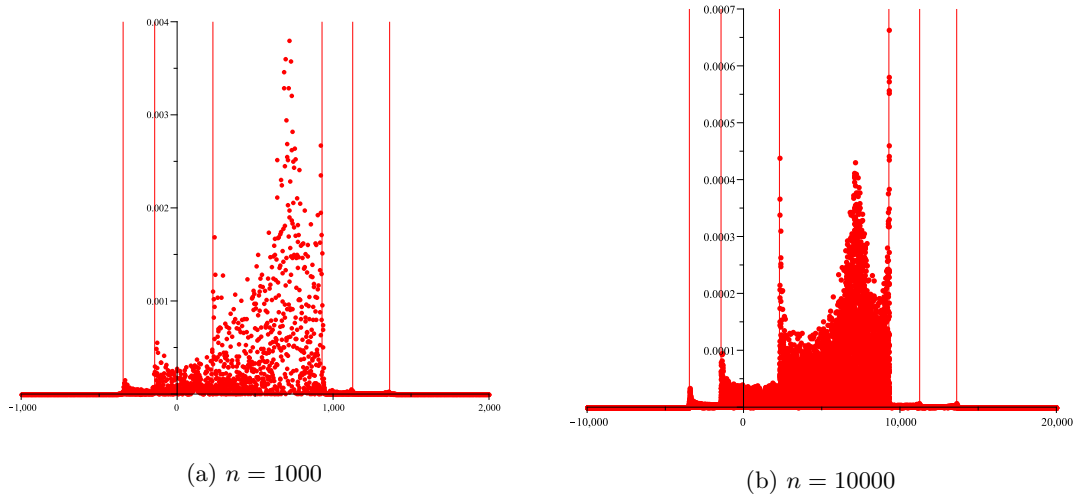


Figure 4.6: As $n \rightarrow \infty$, one peak scales down more rapidly.

a nearly flat spot in figure 4.5b, at height around 0.7. The curve stays nearly horizontal for some time, causing the false peak to remain spread over a macroscopic rescaled region.

4.5 Two-dimensional QRW

In this section we consider two examples of QRW with $d = 2$, $k = 4$ and steps $\mathbf{v}^{(1)} = (0, 0)$, $\mathbf{v}^{(2)} = (1, 0)$, $\mathbf{v}^{(3)} = (0, 1)$ and $\mathbf{v}^{(4)} = (1, 1)$. To complete the specification of the two examples, we give

the two unitary matrices:

$$U_1 := \frac{1}{2} \begin{bmatrix} 1 & 1 & 1 & 1 \\ -1 & 1 & -1 & 1 \\ 1 & -1 & -1 & 1 \\ -1 & -1 & 1 & 1 \end{bmatrix} \quad (4.10)$$

$$U_2 := \frac{1}{2} \begin{bmatrix} 1 & 1 & 1 & 1 \\ -1 & 1 & -1 & 1 \\ -1 & 1 & 1 & -1 \\ -1 & -1 & 1 & 1 \end{bmatrix}. \quad (4.11)$$

Note that these are both Hadamard matrices; neither is the Hadamard matrix with the bound state considered in [Moo04], nor is either in the two-parameter family referred to as Grover walks in [WKKK08]. The second differs from the first in that the signs in the third row are reversed. Both are members of one-parameter families analyzed in [BBBP10], in Sections 4.1 and 4.3 respectively. The (arbitrary) names given to these matrices in [Bra07, BBBP10] are respectively $S(1/2)$ and $B(1/2)$. Intensity plots at time 200 for these two quantum walks, given in figure 4.7, reproduce those taken from [BBBP10] but with different parameter values ($1/2$ each time, instead of $1/8$ and $2/3$ respectively).

For the case of U_1 it is shown in [BBBP10, Lemma 4.3] that \mathcal{V}_1 is smooth. Asymptotics follow, as in Theorem 4.3.3 of the present paper, and an intensity plot of the asymptotics is generated that matches the empirical time 200 plot quite well. In the case of U_2 , \mathcal{V}_1 is not smooth but [BBBP10, Theorem 3.5] shows that the singular points do not contribute to the asymptotics. Again, a limiting intensity plot follows from Theorem 4.3.3 of the present paper and matches the time 200 profile quite well.

It follows from Proposition 4.4.3 that the union of darkened curves where the intensity blows up is the algebraic curve where κ vanishes, and that this includes the boundary of the feasible region.

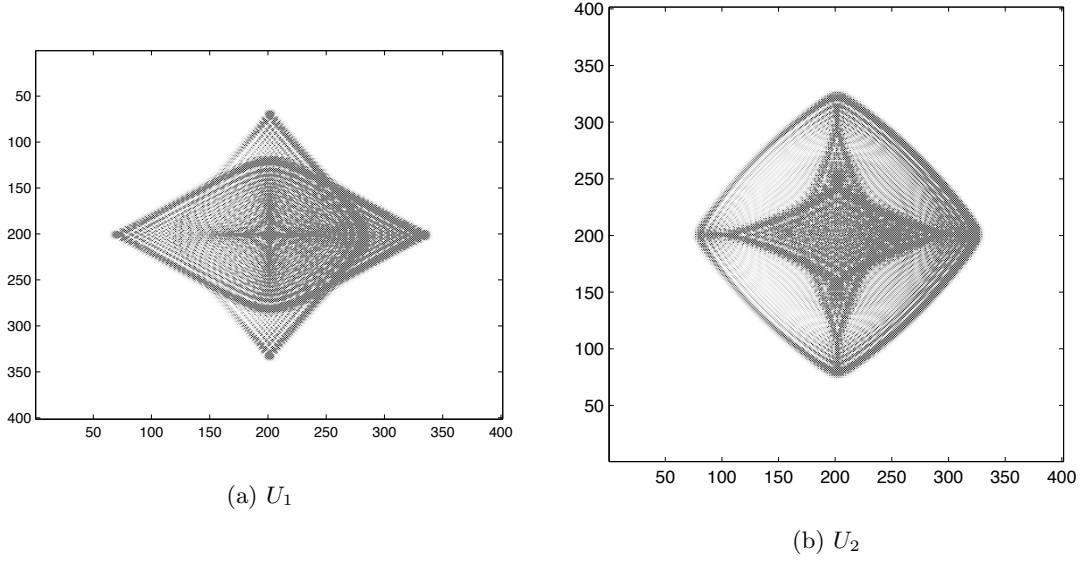


Figure 4.7: Time 200 probability profiles for two quantum walks: the darkness at (r, s) corresponds to the squared amplitude.

The main result of this section is the identification of the algebraic curve. While this result is only computational, it is one of the first examples of computation of such a curve, the only similar prior example being the computation of the “Octic circle” boundary of the feasible region for so-called diabolos tilings, identified without proof by Cohn and Pemantle and first proved by [KO07] (see also [BP10]). The perhaps somewhat comical statement of the result is as follows.

Theorem 4.5.1. *For the quantum walk with unitary coin flip U_2 , the curvature of the variety \mathcal{V}_1 vanishes at some $\mathbf{z} \in Z(r, s)$ if and only if (r, s) is a zero of the polynomial P_2 and satisfies $|r| + |s| < 3/4$, where*

$$\begin{aligned}
P_2(r, s) := & 1 + 14r^2 - 3126r^4 + 97752r^6 - 1445289r^8 + 12200622r^{10} - 64150356r^{12} + 220161216r^{14} - \\
& 504431361r^{16} + 774608490r^{18} - 785130582r^{20} + 502978728r^{22} \\
& - 184298359r^{24} + 29412250r^{26} + 14s^2 - 1284r^2s^2 - 113016r^4s^2 + 5220612r^6s^2 - \\
& 96417162r^8s^2 + 924427224r^{10}s^2 - 4865103360r^{12}s^2 + 14947388808r^{14}s^2 - \\
& 27714317286r^{16}s^2 + 30923414124r^{18}s^2 - 19802256648r^{20}s^2 + 6399721524r^{22}s^2 -
\end{aligned}$$

$$\begin{aligned}
& 721963550r^{24}s^2 - 3126s^4 - 113016r^2s^4 + 7942218r^4s^4 - 68684580r^6s^4 - 666538860r^8s^4 + 15034322304r^{10}s^4 - \\
& 86727881244r^{12}s^4 + 226469888328r^{14}s^4 - 296573996958r^{16}s^4 + 183616180440r^{18}s^4 - 32546593518r^{20}s^4 - \\
& 8997506820r^{22}s^4 + 97752s^6 + 5220612r^2s^6 - 68684580r^4s^6 + 3243820496r^6s^6 - 25244548160r^8s^6 + \\
& 59768577720r^{10}s^6 - \\
& 147067477144r^{12}s^6 + 458758743568r^{14}s^6 - 749675452344r^{16}s^6 + 435217945700r^{18}s^6 - 16479111716r^{20}s^6 - \\
& 1445289s^8 - 96417162r^2s^8 - 666538860r^4s^8 - 25244548160r^6s^8 + 194515866042r^8s^8 - 421026680628r^{10}s^8 + \\
& 611623295476r^{12}s^8 - \\
& 331561483632r^{14}s^8 + 7820601831r^{16}s^8 + 72391117294r^{18}s^8 + 12200622s^{10} + \\
& 924427224r^2s^{10} + 15034322304r^4s^{10} + 59768577720r^6s^{10} - 421026680628r^8s^{10} + \\
& 421043188488r^{10}s^{10} - 1131276050256r^{12}s^{10} - 196657371288r^{14}s^{10} + \\
& 151002519894r^{16}s^{10} - 64150356s^{12} - 4865103360r^2s^{12} - 86727881244r^4s^{12} - \\
& 147067477144r^6s^{12} + 611623295476r^8s^{12} - 1131276050256r^{10}s^{12} + 586397171964r^{12}s^{12} - 231584205720r^{14}s^{12} + \\
& 220161216s^{14} + 14947388808r^2s^{14} + 226469888328r^4s^{14} + \\
& 458758743568r^6s^{14} - 331561483632r^8s^{14} - 196657371288r^{10}s^{14} - 231584205720r^{12}s^{14} - 504431361s^{16} - \\
& 27714317286r^2s^{16} - 296573996958r^4s^{16} - 749675452344r^6s^{16} + \\
& 7820601831r^8s^{16} + 151002519894r^{10}s^{16} + 774608490s^{18} + 30923414124r^2s^{18} + \\
& 183616180440r^4s^{18} + 435217945700r^6s^{18} + 72391117294r^8s^{18} - 785130582s^{20} - \\
& 19802256648r^2s^{20} - 32546593518r^4s^{20} - 16479111716r^6s^{20} + 502978728s^{22} + \\
& 6399721524r^2s^{22} - 8997506820r^4s^{22} - 184298359s^{24} - 721963550r^2s^{24} + 29412250s^{26}.
\end{aligned}$$

We check visually that the zero set of P_2 does indeed coincide with the curves of peak intensity for the U_2 QRW.

Before embarking on the proof, let us be clear about what is required. If \mathbf{r} is in the boundary of the feasible region, then κ must vanish at the pre-images of \mathbf{r} in the unit torus. The boundary, ∂G , of the feasible region is therefore a component of a real algebraic variety, W . The variety W is the image under the logarithmic Gauss map μ of the points of the unit torus where Q and κ both vanish. Computing this variety is easy in principle: two algebraic equations in (x, y, z, r, s)

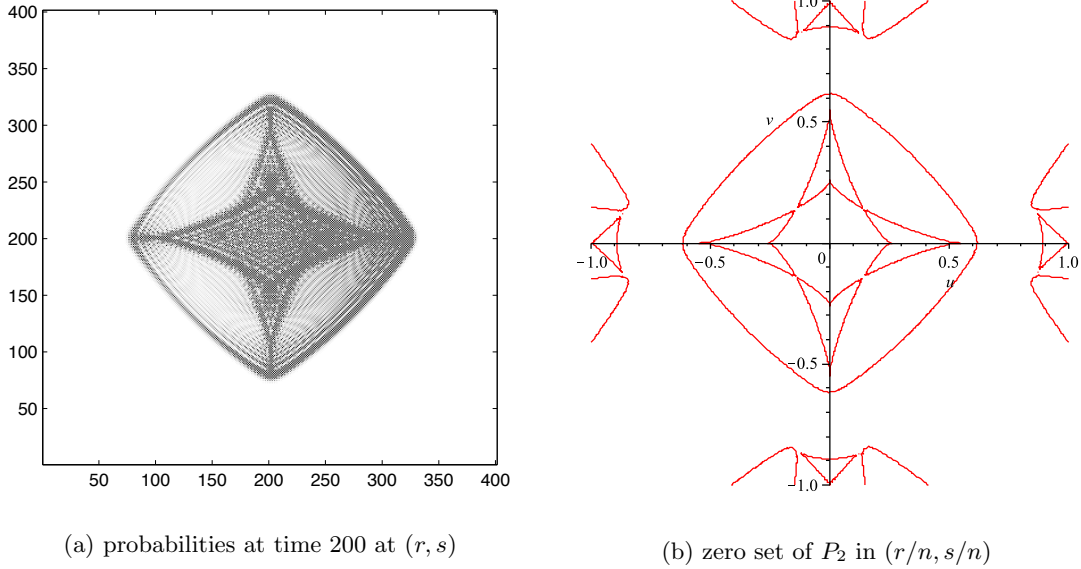


Figure 4.8: The probability profile for the U_2 QRW alongside the graph of the zero set of P_2 .

give the conditions for $\mu(x, y, z) = (r, s)$ and two more give conditions for $Q(x, y, z) = \kappa(x, y, z) = 0$; algebraically eliminating $\{x, y, z\}$ then gives the defining polynomial P_2 for W . In fact, due to the number of variables and the degree of the polynomials, a straightforward Gröbner basis computation does not work and we need to use iterated resultants in order to get the computation to halt. The last step is to discard extraneous real zeros of P_2 , namely those in the interior of G or G^c , so as to arrive at a precise description of ∂G .

Proof. To eliminate subscripts, we use the variables (x, y, z) instead of (x_1, x_2, y) . The condition for $\mathbf{z} \in Z(r, s)$ is given by the vanishing of two polynomials H_1 and H_2 in (x, y, z, r, s) , where

$$\begin{aligned}
 H_1(x, y, z, r, s) &:= xQ_x - rzQ_z; \\
 H_2(x, y, z, r, s) &:= yQ_y - szQ_z.
 \end{aligned}$$

The curvature of \mathcal{V}_1 at \mathbf{z} also vanishes when a single polynomial vanishes, which we will call $L(x, y, z)$. We derive an explicit formulae for L : For $(x, y, z) \in \mathcal{V}_1$, write $x = e^{iX}$, $y = e^{iY}$ and $z = e^{iZ}$. By Proposition 4.4.1 we know that $Q_z \neq 0$ on \mathcal{V}_1 , hence the parametrization of \mathcal{V}_1 by X

and Y near a point (x, y, z) is smooth and the partial derivatives $Z_X, Z_Y, Z_{XX}, Z_{XY}, Z_{YY}$ are well defined. Implicitly differentiating $Q(e^{iX}, e^{iY}, e^{iZ(X,Y)}) = 0$ with respect to X and Y we obtain

$$Z_X = -\frac{xQ_x}{zQ_z} \quad \text{and} \quad Z_Y = -\frac{yQ_y}{zQ_z},$$

and differentiating again yields

$$\begin{aligned} Z_{XX} &= \frac{-ixz}{(zQ_z)^3} [Q_x Q_z (zQ_z - 2xzQ_{xz} + xQ_x) + xz(Q_x^2 Q_{zz} + Q_z^2 Q_{xx})]; \\ Z_{YY} &= \frac{-iyz}{(zQ_z)^3} [Q_y Q_z (zQ_z - 2yzQ_{yz} + zQ_y) + yz(Q_y^2 Q_{zz} + Q_z^2 Q_{yy})]; \\ Z_{XY} &= \frac{-ixyz}{(zQ_z)^3} [zQ_z(Q_z Q_{xy} - Q_x Q_{yz} - Q_y Q_{xz}) + Q_x Q_y Q_z + zQ_x Q_y Q_{zz}]. \end{aligned}$$

In any dimension, the Gaussian curvature vanishes exactly when the determinant of the Hessian vanishes of any parametrization of the surface as a graph over $d - 1$ variables. In particular, the curvature vanishes when

$$\det \begin{pmatrix} Z_{XX} & Z_{XY} \\ Z_{XY} & Z_{YY} \end{pmatrix}$$

vanishes, and plugging in the computed values yields the polynomial

$$\begin{aligned} L(x, y, z) &:= -xyzQ_z^2 Q_{xy}^2 + zQ_x Q_z^2 Q_y - 2yzQ_x Q_z Q_y Q_{yz} + yQ_x Q_z Q_y^2 + yzQ_x Q_y^2 Q_{zz} \\ &+ yzQ_x Q_z^2 Q_{yy} - 2xzQ_x Q_z Q_{xz} Q_y + 2xyzQ_x Q_{xz} Q_y Q_{yz} - 2xyzQ_x Q_z Q_{xz} Q_{yy} \\ &+ xQ_x^2 Q_z Q_y + xyQ_x^2 Q_z Q_{yy} + xzQ_x^2 Q_{zz} Q_y + xyzQ_x^2 Q_{zz} Q_{yy} + xzQ_{xx} Q_z^2 Q_y \\ &- 2xyzQ_{xx} Q_z Q_y Q_{yz} + xyQ_{xx} Q_z Q_y^2 + xyzQ_{xx} Q_y^2 Q_{zz} + xyzQ_{xx} Q_z^2 Q_{yy} - xyzQ_y^2 Q_{xz}^2 \\ &- xyzQ_x^2 Q_{yz}^2 + 2xyzQ_z Q_{xy} Q_x Q_{yz} + 2xyzQ_z Q_{xy} Q_y Q_{xz} - 2xyQ_z Q_{xy} Q_x Q_y \\ &- 2xyzQ_{xy} Q_x Q_y Q_{zz}. \end{aligned}$$

It follows that the curvature of \mathcal{V}_1 vanishes for some $(x, y, z) \in Z(r, s)$ if and only if the four polynomials Q, H_1, H_2 and L all vanish at some point (x, y, z, r, s) with $(x, y, z) \in T^3$. Ignoring the condition $(x, y, z) \in T^3$ for the moment, we see that we need to eliminate the variables (x, y, z) from the four equations, leading to a one-dimensional ideal in r and s . Unfortunately Gröbner

$h(x, y_2) = 0$. It follows that if $f(x, y) = g(x, y) = 0$ then $R = 0$, but the converse does not in general hold. A detailed discussion of this may be found in [BM07].

For our purposes, it will suffice to compute iterated resultants and then pass to a subvariety where a common root indeed occurs. We may eliminate repeated factors as we go along. Accordingly, we compute

$$R_{12} := \mathcal{Rad}(\text{result}(Q, L, x))$$

$$R_{13} := \mathcal{Rad}(\text{result}(Q, H_1, x))$$

$$R_{14} := \mathcal{Rad}(\text{result}(Q, H_2, x))$$

where $\mathcal{Rad}(P)$ denotes the product of the first powers of each irreducible factor of P . Maple is kind to us because we have used the shortest of the four polynomials, Q , in each of the three first-level resultants. Next, we eliminate y via

$$R_{124} := \mathcal{Rad}(\text{result}(R_{12}, R_{14}, y))$$

$$R_{134} := \mathcal{Rad}(\text{result}(R_{13}, R_{14}, y)).$$

Polynomials R_{124} and R_{134} each have several small univariate factors, as well as one large multivariate factor which is irreducible over the rationals. Denote the large factors by f_{124} and f_{134} . Clearly the univariate factors do not contribute to the set we are looking for, so we eliminate z by defining

$$R_{1234} := \mathcal{Rad}(\text{result}(f_{124}, f_{134}, z)).$$

Maple halts, and we obtain a single polynomial in the variables (r, s) whose zero set contains the set we are after. Let Ω denote the set of (r, s) such that $\kappa(x, y, z) = 0$ for some $(x, y, z) \in \mathcal{V}$ with $\mu(x, y, z) = (r, s)$ [note: this definition uses \mathcal{V} instead of \mathcal{V}_1 .] It follows from the symmetries of the problem that Ω is symmetric under $r \mapsto -r$ as well as $s \mapsto -s$ and the interchange of r and s . Computing iterated resultants, as we have observed, leads to a large zero set Ω' ; the set Ω' may not possess r - s symmetry, as this is broken by the choice of order of iteration. Factoring the

iterated resultant, we may eliminate any component of Ω' whose image under transposition of r and s is not in Ω' . Doing so, yields the irreducible polynomial P_2 . Because the set Ω is algebraic and known to be a subset of the zero set of the irreducible polynomial P_2 , we see that Ω is equal to the zero set of P_2 .

Let $\Omega_0 \subseteq \Omega$ denote the subset of those (r, s) for which as least one $(x, y, z) \in \mu^{-1}((r, s))$ with $\kappa(x, y, z) = 0$ lies on the unit torus. It remains to check that Ω_0 consists of those $(r, s) \in \Omega$ with $|r| + |s| < 3/4$.

The locus of points in \mathcal{V} at which κ vanishes is a complex algebraic curve γ given by the simultaneous vanishing of Q and L . It is nonsingular as long as ∇Q and ∇L are not parallel, in which case its tangent vector is parallel to $\nabla Q \times \nabla L$. Let $\rho := xQ_x/(zQ_z)$ and $\sigma := yQ_y/(zQ_z)$ be the coordinates of the map μ under the identification of \mathbb{CP}^2 with $\{(r, s, 1) : r, s \in \mathbb{C}\}$. The image of γ under μ (and this identification) is a nonsingular curve in the plane, provided that γ is nonsingular and either $d\rho$ or $d\sigma$ is nonvanishing on the tangent. For this it is sufficient that one of the two determinants $\det M_\rho, \det M_\sigma$ does not vanish, where the columns of M_ρ are $\nabla Q, \nabla L, \nabla \rho$ and the columns of M_σ are $\nabla Q, \nabla L, \nabla \sigma$.

Let (x_0, y_0, z_0) be any point in \mathcal{V}_1 at which one of these two determinants does not vanish. It is shown in [BBBP10, Proposition 2.1] that the tangent vector to γ at (x_0, y_0, z_0) in logarithmic coordinates is real; therefore the image of γ near (x_0, y_0, z_0) is a nonsingular real curve. Removing singular points from the zero set of P_2 leaves a union \mathcal{U} of connected components, each of which therefore lies in Ω_0 or is disjoint from Ω_0 . The proof of the theorem is now reduced to listing the components, checking that none crosses the boundary $|r| + |s| = 3/4$, and checking $Z(r, s)$ for a single point (r, s) on each component (note: any component intersecting $\{|r| + |s| > 1\}$ need not be checked as we know the coefficients to be identically zero here). \square

We close by stating a result for U_1 , analogous to Theorem 4.5.1. The proof is entirely analogous as well and will be omitted.

Theorem 4.5.2. *For the quantum walk with unitary coin flip U_1 , the curvature of the variety \mathcal{V}_1 vanishes at some $(x, y, z) \in Z(r, s)$ if and only if $|r|$ and $|s|$ are both at most $2/3$ and (r, s) is a zero of the polynomial*

$$\begin{aligned}
P_1(r, s) := & 132019r^{16} + 2763072s^2r^{20} - 513216s^2r^{22} - 6505200s^2r^{18} + 256s^2r^2 + \\
& 8790436s^2r^{16} - 10639416s^{10}r^8 + 39759700s^{12}r^4 - 12711677s^{10}r^4 + 4140257s^{12}r^2 - \\
& 513216s^{22}r^2 - 7492584s^2r^{14} + 2503464s^{10}r^6 - 62208s^{22} + 16s^6 + 141048r^{20} + \\
& 8790436s^{16}r^2 + 2763072s^{20}r^2 - 6505200s^{18}r^2 - 40374720s^{18}r^6 + 64689624s^{16}r^4 - \\
& 33614784s^{18}r^4 + 14725472s^{10}r^{10} + 121508208s^{16}r^8 - 1543s^{10} - 23060s^2r^6 + \\
& 100227200s^{10}r^{12} + 7363872s^{20}r^4 - 176524r^{18} + 121508208s^8r^{16} - 197271552s^8r^{14} - 13374107s^8r^6 + \\
& 1647627s^8r^4 + 18664050s^8r^8 - 227481984s^{10}r^{14} - 19343s^4r^4 + \\
& 279234496s^{12}r^{12} - 67173440s^{14}r^4 - 7492584s^{14}r^2 + 4140257s^2r^{12} + 291173s^2r^8 - \\
& 1449662s^2r^{10} + 7363872s^4r^{20} - 227481984s^{14}r^{10} + 132019s^{16} - 197271552s^{14}r^8 - \\
& 59209r^{14} - 1449662s^{10}r^2 + 100227200s^{12}r^{10} - 1543r^{10} - 153035200s^{14}r^6 - 13374107s^6r^8 + 3183044s^6r^6 + \\
& 39759700s^4r^{12} - 176524s^{18} + 72718s^6r^4 + 1647627s^4r^8 - 62208r^{22} + 141048s^{20} - 1472s^4r^2 + 11664s^{24} - \\
& 33614784s^4r^{18} + 128187648s^{16}r^6 - 1472s^2r^4 - 67173440s^4r^{14} + 291173s^8r^2 + 64689624s^4r^{16} - \\
& 10639416s^8r^{10} - 59209s^{14} + 72718s^4r^6 + 92321584s^8r^{12} - 56r^8 + 92321584s^{12}r^8 - 153035200s^6r^{14} - \\
& 23060s^6r^2 + 128187648s^6r^{16} - 40374720s^6r^{18} + 72282208s^{12}r^6 + 14793r^{12} + 11664r^{24} + 14793s^{12} + \\
& 16r^6 + 2503464s^6r^{10} - 56s^8 - 12711677s^4r^{10} + 72282208s^6r^{12}.
\end{aligned}$$

4.6 Next Steps

4.6.1 Higher dimensions

As with the development of the one-dimensional case in Section 4.2.2, the two-dimensional QRWs can be generalized beyond the Hadamard walk similarly. Our online database mentioned above includes several 2-dimensional walks. For example, we can take a walk with the same 4 chiralities

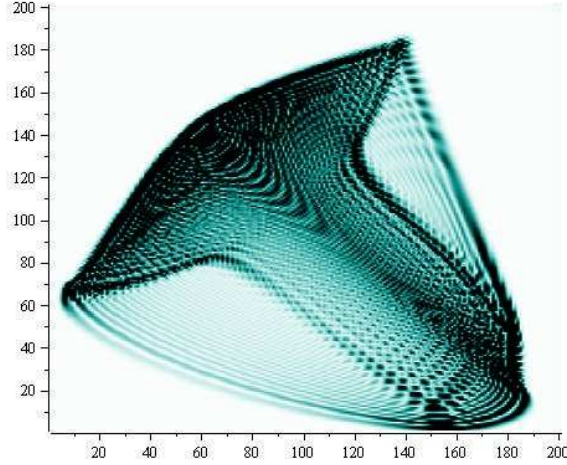


Figure 4.9: The probability distribution of a 2-dimensional QRW after 200 steps.

as above, $\{(0, 1), (0, -1), (1, 0), (-1, 0)\}$, the unitary matrix

$$U := \begin{pmatrix} \frac{57}{67} & -\frac{12}{67} & \frac{30}{67} & \frac{14}{67} \\ \frac{204}{469} & \frac{17}{469} & -\frac{30}{67} & -\frac{366}{469} \\ -\frac{10}{469} & \frac{390}{469} & \frac{33}{67} & -\frac{120}{469} \\ \frac{138}{469} & \frac{246}{469} & -\frac{40}{67} & \frac{249}{469} \end{pmatrix},$$

and a starting distribution of the particle with amplitude $\frac{1}{\sqrt{2}}$ in each of the first two chiralities. After 200 steps, we get the distribution in Figure ??, where as above, darker spots represent higher probabilities of the particle ending in that location.

Similarly, we can extend the process to 3 or more dimensions. For 3 dimensions, we choose the chiralities $\{(0, 0, 1), (0, 0, -1), (0, 1, 0), (0, -1, 0), (1, 0, 0), (-1, 0, 0)\}$ with a starting state in the

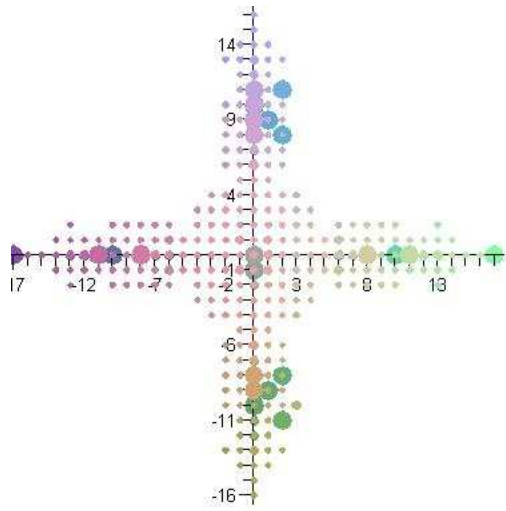
first chirality, and the unitary matrix

$$\begin{vmatrix} -\frac{2}{3} & \frac{1}{3} & \frac{1}{3} & \frac{1}{3} & \frac{1}{3} & \frac{1}{3} \\ \frac{1}{3} & -\frac{2}{3} & \frac{1}{3} & \frac{1}{3} & \frac{1}{3} & \frac{1}{3} \\ \frac{1}{3} & \frac{1}{3} & -\frac{2}{3} & \frac{1}{3} & \frac{1}{3} & \frac{1}{3} \\ \frac{1}{3} & \frac{1}{3} & \frac{1}{3} & -\frac{2}{3} & \frac{1}{3} & \frac{1}{3} \\ \frac{1}{3} & \frac{1}{3} & \frac{1}{3} & \frac{1}{3} & -\frac{2}{3} & \frac{1}{3} \\ \frac{1}{3} & \frac{1}{3} & \frac{1}{3} & \frac{1}{3} & \frac{1}{3} & -\frac{2}{3} \end{vmatrix}$$

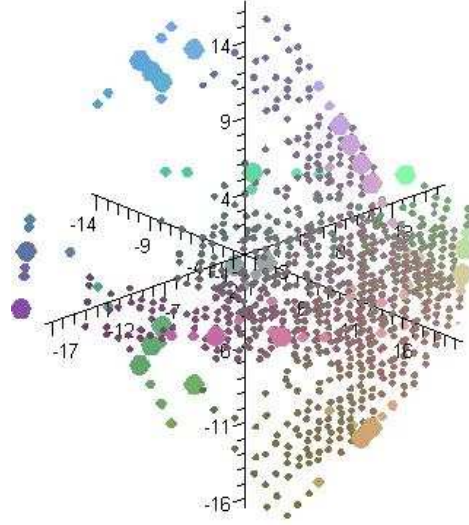
After twenty steps, we obtain the three-dimensional probability distribution Figure 4.10, where the size of the ball represents the probability it is at that point.

4.6.2 Multiple peaks

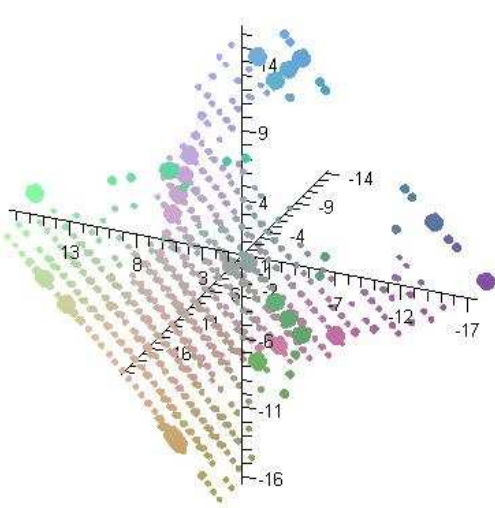
Finally, the QRW database has shown that the number of peaks for a given QRW with the same chiralities and initial state is not independent of the matrix, U . Therefore, we would like to investigate what controls the number of peaks. Say that the two QRWs have unitary matrices U_1 and U_2 . One possible technique to compare the two is to use the inverse of the map from skew-hermitian matrices to unitary matrices described above, in order to find 2 skew-hermitian matrices S_1 and S_2 which correspond to U_1 and U_2 , respectively. Then, we can create a parameter t in a skew-hermitian matrix H such that at time $t = 0$, $H = S_1$, and at time $t = 1$, $H = S_2$. Through the forward map once again, this parameterization then describes a continuous family of unitary matrices, and therefore a family of QRWs which have a varying number of peaks. Upon further analyzation, it should be possible to identify exact values of t where the QRW switches between numbers of peaks, representing critical QRWs with “double peaks” or other new phenomena. To date, these computations have been too complex to halt in Maple.



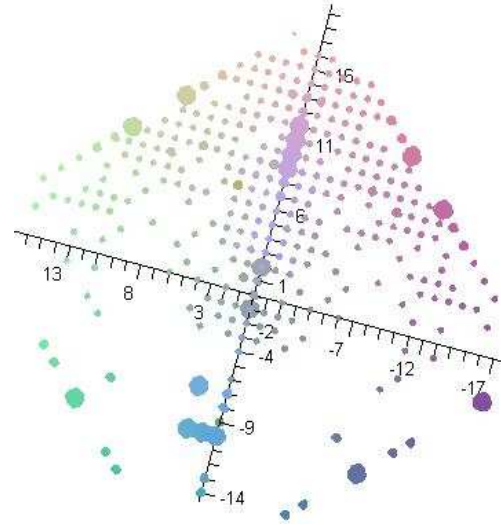
(a)



(b)



(c)



(d)

Figure 4.10: A 3-dimensional QRW after 20 steps.

Bibliography

- [ABN⁺01] A. Ambainis, E. Bach, A. Nayak, A. Vishwanath, and J. Watrous, *One-dimensional quantum walks*, Proceedings of the 33rd Annual ACM Symposium on Theory of Computing (New York), ACM Press, 2001, pp. 37-49.
- [ADZ93] Y. Aharonov, L. Davidovich, and N. Zagury, *Quantum random walks*, Phys. Rev. A **48** (1993), pp. 1687-1690.
- [BBBP10] Y. Baryshnikov, W. Brady, A. Bressler, and R. Pemantle, *Two-dimensional quantum random walk*, J. Stat. Phys., vol 142 (2010), pp. 78-107.
- [BP10] Y. Baryshnikov and R. Pemantle, *The “octic circle” theorem for diabolos tilings: a generating function with a quartic singularity*, Manuscript in progress (2010).
- [BP11] Y. Baryshnikov and R. Pemantle. *Asymptotics of multivariate sequences, part III: quadratic points*. In Adv. Math., vol 228 (2011) pp. 3127-3206. Available online:
<http://www.math.upenn.edu/~pemantle/papers/cones.pdf>
- [BR83] E.A. Bender and L.B. Richmond. *Central and local limit theorems applied to asymptotic enumeration. II. Multivariate generating functions*. In J. Combin. Theory Ser. A, vol 34 (1983) pp. 255-265.
- [Bra07] W. Brady, *Quantum random walks on \mathbb{Z}^2* , Master of Philosophy Thesis, the University of Pennsylvania (2007).

- [BGPP09] Andrew Bressler, Torin Greenwood, Robin Pemantle, and Marko Petkovšek. Quantum random walk on the integer lattice: examples and phenomena. **arXiv**, math-ph/0903.2967v2 (2009), 18. To appear in the Proceedings of the AMS, in the Special Sessions on Algorithmic Probability and Combinatorics. Edited by Manuel E. Lladser, Robert S. Maier, Marni Mishna, and Andrew Rechnitzer.
- [BP07] A. Bressler and R. Pemantle, *Quantum random walks in one dimension via generating functions*, Proceedings of the 2007 Conference on the Analysis of Algorithms, vol. AofA 07, LORIA, Nancy, France, 2007, p. 11.
- [BCA03] Todd A. Brun, Hilary A. Carteret, and A. Ambainis, *Quantum walks driven by many coins*, Phys. Rev. A **67** (2003), no. 5.
- [BM07] L. Busé and B. Mourrain, *Explicit factors of some iterated resultants and discriminants*, arXiv:CS **0612050** (2007), 42.
- [CIR03] Hilary A. Carteret, Mourad E. H. Ismail, and Bruce Richmond, *Three routes to the exact asymptotics for the one-dimensional quantum walk*, J. Phys. A **36** (2003), 8775-8795.
- [CLO98] D. Cox, J. Little, and D. O’Shea, *Using algebraic geometry*, Graduate Texts in Mathematics, vol. 185, Springer-Verlag, Berlin, 1998.
- [DeV10] T. DeVries, *A case study in bivariate singularity analysis*. In Algorithmic Probability and Combinatorics, Cont. Math. vol. 520 (2011), pp. 61-82.
- [DeV11] T. DeVries, *Algorithms for Bivariate Singularity Analysis*, Doctor of Philosophy Thesis, the University of Pennsylvania (2011).
- [DVvdHP11] DeVries, T., van der Hoeven, J. and Pemantle, R., *Automatic asymptotics for coefficients of smooth, bivariate rational functions*, Online J. Anal. Comb., vol. 6 (2011), 24 pages.

- [FO90] P. Flajolet and A. M. Odlyzko. *Singularity analysis of generating functions*. In SIAM J. Discrete Math., vol 3 (1990) pp. 216-240. Available online:
<http://algo.inria.fr/flajolet/Publications/F10d90b.pdf>
- [GR92] Z. Gao and L.B. Richmond. *Central and local limit theorems applied to asymptotic enumeration. IV. Multivariate generating functions*. In J. Comput. Appl. Math., vol 41 (1992) pp. 177-186.
- [GKZ94] I. Gelfand, M. Kapranov, and A. Zelevinsky, *Discriminants, resultants and multidimensional determinants*, Birkh auser, Boston-Basel-Berlin, 1994.
- [GM88] M. Goresky and R. MacPherson. *Stratified Morse Theory*, Springer-Verlag, Berlin Heidelberg, 1988. Available online: <http://www.math.ias.edu/~goresky/MathPubl.html>
- [Hwa96] Hwang, H.-K. *Large deviations for combinatorial distributions. I. Central limit theorems*. In Ann. Appl. Probab., vol 6 (1996) pp. 297-319. Available online:
http://projecteuclid.org/download/pdf_1/euclid.aop/1034968075
- [Hwa98] Hwang, H.-K. *Large deviations for combinatorial distributions. II. Local limit theorems*. In Ann. Appl. Probab., vol 8 (1998) pp. 163-181. Available online:
http://projecteuclid.org/download/pdf_1/euclid.aop/1027961038
- [IKK04] N. Innui, Y. Konishi, and N. Konno, *Localization of two-dimensional quantum walks*, Physical Review A **69** (2004), 052323-1 - 052323-9.
- [KEM05] J. Kempe, *Quantum random walks - an introductory overview*, Contemporary Physics, Vol. 44 (13 Mar 2003), pp. 307-327.
- [Ken07] V. Kendon, *Decoherence in quantum walks - a review*, Comput. Sci. **17(6)** (2007), 1169-1220.

- [KO07] R. Kenyon and A. Okounkov, *Limit shapes and the complex burgers equation*, Acta Math. **199** (2007), 263-302.
- [IKS05] N. Inui, N. Konno, and E. Segawa, *One-dimensional three-state quantum walk*, Phys. Rev. E **72**, 056112 (Nov 2005), 7 pages.
- [Kon08] N. Konno, *Quantum random walks for computer scientists*, Quantum Potential Theory, Springer-Verlag, Heidelberg, 2008, pp. 309-452.
- [LO91] H. Liebeck and A. Osborne, *The generation of all rational orthogonal matrices*, Amer. Math. Monthly **98** (1991), no. 2, 131-133.
- [MBSS02] T. Mackay, S. Bartlett, L. Stephanson, and B. Sanders, *Quantum walks in higher dimensions*, Journal of Physics A **35** (2002), 2745-2754.
- [Mey96] D. Meyer, *From quantum cellular automata to quantum lattice gases*, Journal Stat. Phys. **85** (1996), 551-574.
- [Moo04] Cristopher Moore, *e-mail from Cris Moore on quantum walks*, Domino Archive (2004).
- [PW02] R. Pemantle and M. Wilson. *Asymptotics of multivariate sequences, part I: smooth points of the singular variety*. In J. Comb. Theory, Series A,, vol 97 (2002) pp. 129-161. Available online:
<http://www.math.upenn.edu/~pemantle/papers/p1.pdf>
- [PW04] R. Pemantle and M. Wilson. *Asymptotics of multivariate sequences, part II: multiple points of the singular variety*. In Combinatorics, Probability and Computing, vol 13, no. 4 (2004) pp. 735-761. Available online: <http://www.math.upenn.edu/~pemantle/papers/multiplepoints.pdf>

- [PW13] R. Pemantle and M. Wilson. *Analytic Combinatorics in Several Variables*, Cambridge University Press, New York, 2013. Available online: <http://www.math.upenn.edu/~pemantle/ACSV.pdf>
- [VA08] S.E. Venegas-Andraca, *Quantum walks for computer scientists*, Synthesis Lectures on Quantum Computing, Morgan and Claypool, San Rafael, CA, 2008.
- [Wil06] H.S. Wilf. *generatingfunctionology*. Academic Press Inc., Boston, second edition, 1994.
- [WKKK08] K. Watabe, N. Kobayashi, M. Katori, and N. Konno, *Limit distributions of two-dimensional quantum walks*, Physical Review A **77** (2008), 062331-1 - 062331-9.